

## 5.0 Summary and Conclusions

To develop high temperature facilitated membranes for the removal of H<sub>2</sub>S from IGCC gas mixtures, three basic experimental activities were pursued:

- (1) evaluation of the H<sub>2</sub>S chemistry of a variety of alkali and alkaline earth carbonate salt mixtures
- (2) development of microporous ceramic materials which were chemically and physically compatible with molten carbonate salt mixtures under IGCC conditions and which could function as a host to support a molten carbonate mixture and
- (3) fabrication of molten carbonate/ceramic immobilized liquid membranes and evaluation of these membranes under conditions approximating those found in the intended application.

A variety of carbonate mixtures consisting of alkali and alkaline earth carbonate salts could be prepared. Characterization by TGA and DTA have shown that seven of these have melting points below 600°C and are essentially nonvolatile under CO<sub>2</sub> at temperatures to 840°C. Of these, four mixtures containing Rb<sub>2</sub>CO<sub>3</sub>, Cs<sub>2</sub>CO<sub>3</sub>, SrCO<sub>3</sub>, or BaCO<sub>3</sub> have apparently not been prepared or characterized previously. The low melting points of the above mixtures relative to pure carbonate salts and their involatility at high temperature make them potentially useful for fabrication of immobilized liquid membranes which selectively permeate H<sub>2</sub>S. In addition, the wide variety of carbonate compositions prepared offers the potential for a range of reactivities with H<sub>2</sub>S.

The properties of one mixture, designated as the base composition (25.2 mole % K<sub>2</sub>CO<sub>3</sub>, 25.7 mole % CaCO<sub>3</sub> in Li<sub>2</sub>CO<sub>3</sub>), were further evaluated. Incorporation of up to 25 mole % sulfide ion into the base composition carbonate mixture resulted in mixtures which were molten at 600°C or lower. That sulfide-containing mixtures are liquid at reasonable temperatures is critical to the success of molten carbonate membranes for removal of H<sub>2</sub>S. Partial solidification of the melt could result in membrane failure. It would appear that the base composition mixture will not suffer from such membrane failure.

Since carbonate membranes permeate H<sub>2</sub>S by a facilitated transport mechanism, a knowledge of the reactivity of H<sub>2</sub>S with the carbonate mixtures described above was required for choice of the optimal membrane material. For this reason, an evaluation of the equilibrium constant for the reaction of the base composition carbonate mixture with H<sub>2</sub>S was carried out by a series of absorption experiments. This activity was complicated by several experimental difficulties. These included gas phase reactivity and the accurate determination of the concentration of water in the gas phase. In addition, at the high temperatures of these experiments, significant reactivity between H<sub>2</sub>S and the absorption vessel and its internal components was observed. This is a very serious problem since some of the H<sub>2</sub>S thought to be absorbed by the melt was actually consumed by reaction with metal. It is unlikely that accurate equilibrium constants were

obtained under such conditions. However, in one experiment, an equilibrium constant for H<sub>2</sub>S absorption was determined, 0.235 atm at 560°C, which was reasonable when compared with literature data.

Through a process involving literature searches and screening experiments, it was determined that aluminum nitride and lithium aluminate were the best candidate ceramics for use as microporous supports for immobilized molten alkali carbonate membranes. Golden Technologies Company, Inc. was successful in producing aluminum nitride discs and tubes with pore sizes in the range 0.38-0.42 μm with 45-50% open porosity. These discs and tubes were infiltrated with molten alkali carbonates at APCI using techniques developed for this program. In the course of this work, it was determined that boron nitride can be used as a coating to help control the infiltration process of these materials. While lithium aluminate has better long term stability than aluminum nitride in contact with the molten alkali carbonates, neither APCI nor Golden Technologies were able to fabricate discs of this material with pore sizes in the range required to contain the molten salts. This was because of limited source suppliers of lithium aluminate powders and the inability to reduce the starting particle size of commercially available powders without introducing excessive mill/media contamination.

Three types of molten carbonate membranes were prepared. These consisted of the base composition carbonate mixture immobilized in a microporous gold frit, a planar microporous ceramic support, or a tubular microporous ceramic support. A significant problem in membrane testing was the tendency of planar ceramic membranes to crack upon sealing in the membrane cell. Membrane cracking was minimized by sealing using a graphite tape technique developed at RTI. Testing of molten carbonate membranes at 560°C and using H<sub>2</sub>S containing feeds at relatively low flow rates was complicated greatly by the reactivity of H<sub>2</sub>S with the membrane cell. As for the absorption experiments above, consumption of H<sub>2</sub>S by reaction with metal led to unreliable determinations of H<sub>2</sub>S permeabilities. This is a serious problem which should be addressed in future work. Membrane cells could be constructed of quartz or alumina which were shown to be inert with respect to H<sub>2</sub>S at temperatures to 700°C. Finally, to be practical, thinner ceramic supports need to be constructed to produce membranes with higher H<sub>2</sub>S fluxes.

Due to the problem of H<sub>2</sub>S-metal reactivity, molten carbonate/planar ceramic membranes were evaluated using feeds which contained no H<sub>2</sub>S. For most of the membranes so examined, gas permeances were quite high indicative of defects in the molten carbonate layer. This is, of course, a serious problem which needs to be addressed further. However, for a few membranes, reasonable, but still somewhat high, CO<sub>2</sub> permeabilities; for example 1,200 Barrers, were obtained suggesting that the fabrication of largely defect free membranes is possible.

Some of the difficulties of H<sub>2</sub>S-metal reactivity were minimized through testing at RTI carried out at significantly higher gas flow rates. Permselective testing was performed using membranes containing the base composition carbonate mixture in planar and

tubular ceramic supports. A more detailed listing of conclusions is provided in the attached RTI final report. The most significant points are summarized below.

Erratic membrane performance was observed. Often, H<sub>2</sub> or He permeabilities were much higher than those predicted based on a solution-diffusion mechanism indicative of defects in the molten carbonate layer. However, in some instances H<sub>2</sub>S to H<sub>2</sub> or He selectivities greater than one were observed. Based on fairly limited data, an observed decrease in H<sub>2</sub>S permeability with increasing feed pressure was consistent with facilitated transport of H<sub>2</sub>S. Examination of membranes after testing revealed that there apparently is a tendency for the melt to migrate in or out of the support. This was particularly apparent for tubular membranes where the salt appeared to have migrated downward along the tube. Planar ceramic membranes examined after testing showed evidence of regions of unfilled pores near the middle of the discs. In addition, for one unused planar ceramic membrane, similar unfilled regions were also observed. Although the experimental information described in this report has not resulted in a demonstration of the use of molten carbonate membrane for removal of H<sub>2</sub>S from fuel gas mixtures, it has shown some success on the way to this goal and has identified the significant problems would need to be addressed by future efforts. These are:

- Minimize or eliminate the reactivity of H<sub>2</sub>S with membrane testing apparatus by using materials of construction (eg. alumina, quartz) which are inert with respect to H<sub>2</sub>S.
- Fabricate ceramic supports which are at least an order of magnitude thinner, or larger in area, than the current ones.
- Address the question of salt migration within the ceramic support.
- Develop techniques for fabricating largely defect-free molten carbonate membranes (e.g. porous structure of support).
- Conduct absorption experiments to evaluate the reactivity of H<sub>2</sub>S with the molten carbonate mixtures identified in this study by using an H<sub>2</sub>S- inert apparatus.
- Develop improved ceramic support materials (e.g. LiAlO<sub>2</sub>) and fabrication methods (to ensure appropriate pore size distribution).

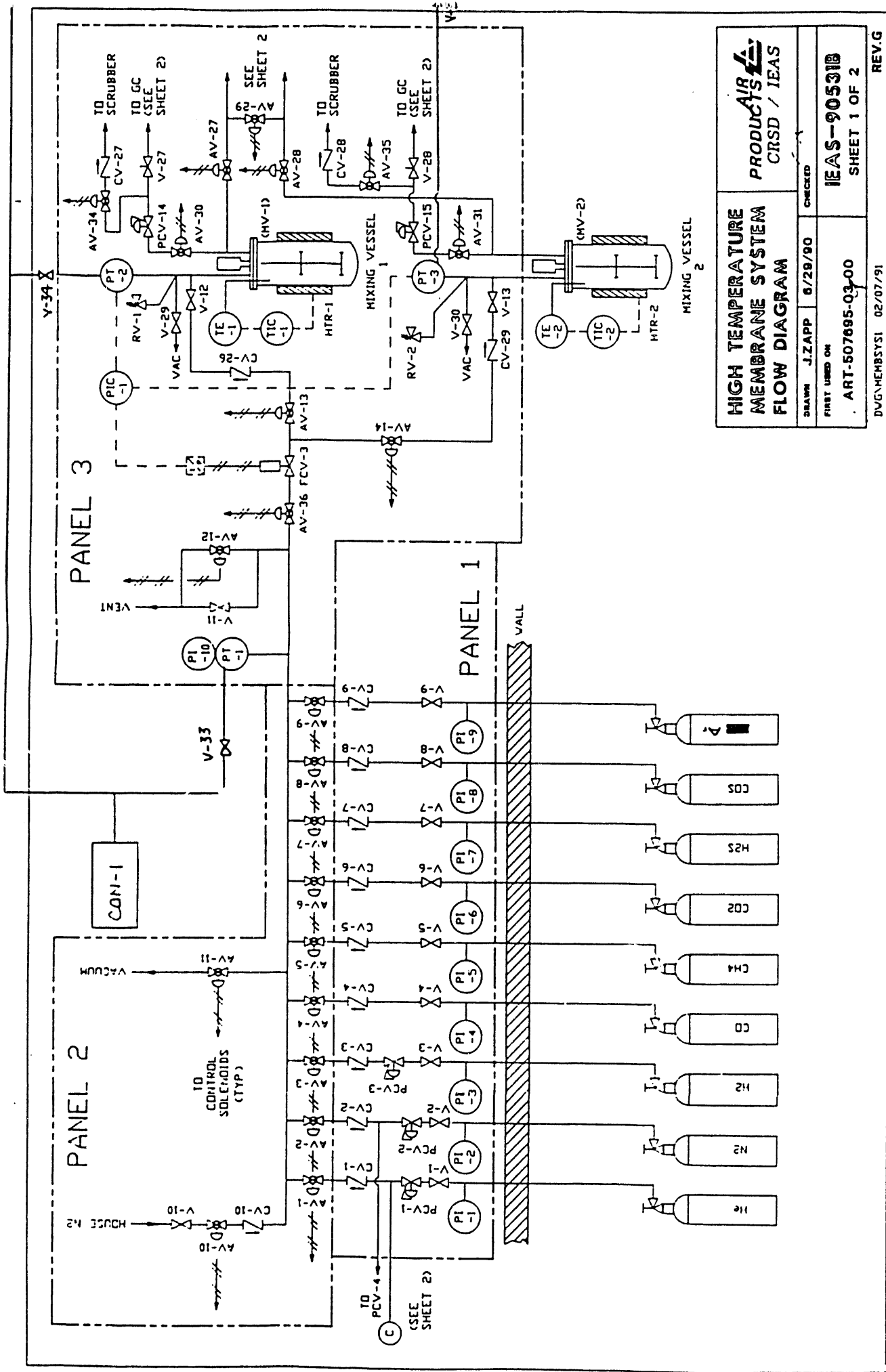
## 6.0 References

1. Cicero, D.C.; Jarr, L.A. *Sep. Sci. Tech.* **25**, 1455-1472 (1990).
2. Robeson, L.M. *J. Mem. Sci.* **62**, 165-85 (1991).
3. Lin, C.L.; Flowers, D.L.; Wu, J.C.S., Smith, G.W.; Liu, P.K.T. "Gas Separation Using Ceramic Membranes" *Proceedings of the Twelfth Annual Gasification and Gas Stream Cleanup Systems Contractors Review Meeting, Volume II*; Johnson, R.A. and Jain, S.C., eds; p.351-361 (1992).
4. Noble, R.D.; Koval, C.A.; Pellegrino, J.J. *Chem. Eng. Progress* **48**, 58-70 (1989).
5. Quinn, R.; Appleby, J.B.; Pez, G.P. U.S. Patent 4,780,114 (1988).
6. Lyke, S.E.; Sealock, L.J. *Proc. Electrochem. Soc.* **84**, 6389-648 (1984).
7. H. C. Maru in "Molten Salt Techniques", Vol. 2; Gale, R.J. and Lovering, D.G., eds.; Plenum Press; p. 15-42 (1984).
8. Moore, R.H.; Schiefelbein, G.F.; Stegen, G.E., "Molten Salt Scrubbing Process for Removal of Particles and Sulfur Compounds from Low Btu Fuel Gases" BNWL-SA-6030, Pacific Northwest lab., Richland, Washington.
9. Stegen, G.E., "Development of Solid Absorption Process for Removal of Sulfur from Fuel Gas". DOE/ET/11028-9 (1982).
10. Lyke, S.E.; Sealock, L.J.; Roberts, G.L., "Development of a Hot Gas Cleanup System for Integrated Coal Gasification/Molten Carbonate Fuel Cell Power Plants", Final Report DOE/MC/19077--1830 (1985).
11. Moore, R.H.; Stegen, G.E. U.S. Patent 4,086,323 (1978).  
Erickson, D.C. U.S. Patent 4,173,619 (1979).
12. Correction for the minor amount of H<sub>2</sub>S consumed to form COS led to no significant change the calculated quantity of H<sub>2</sub>S absorbed by melt.
13. Barin, I.; Knacke, O., "Thermochemical Properties of Inorganic Substances", Springer-Verlag (1973).
14. Webb, T.L.; Kruger, J.E. in "Differential Thermal Analysis" MacKenzie, R.C., editor, Vol. 1, Academic Press, p. 302-341 (1970).
15. *Handbook of Chemistry and Physics*, 71st Edition; Lide, D.R. editor, p. 4-41 to 4-119 (1990)
16. Salarzadeh, I; Tariq, S.A. *Aust. J. Chem.* **36**, 25-31 (1983).
17. Babcock, K.; Winnick, J. *J. Chem. Eng. Data.* **33**, 96-98 (1988).
18. Yosim, S.J.; Grantham, L.F.; McKenzie, D.E.; Stegmann, G.C. *Adv in Chem. Series*, 174-182, Vol. 127 (1973).
19. Nakamoto, K. "Infrared and Raman Spectra of Inorganic and Coordination Compounds" p. 240 (1978).
20. As noted below, it is likely that H<sub>2</sub>O is also present in the gas phase
21. Newsome, D.S. *Catl. Rev.-Sci. Eng.* **21**, 275-318 (1980).
22. T. T. Coyle, T. M. Thomas, and P. Schiessel, "The Corrosion of Materials in Molten Alkali Carbonate Salts at 900°C", SERI/TR025502553, 1985.
23. J. R. Selman and H. C. Maru, *Physical Chemistry of Alkali Carbonate Melts in Advances in Molten Salt Chemistry, Volume 4*, ed. G. Mamantov and J. Braunstein, 159-390. New York: Plenum Press 1981.

24. P. Singh, Corrosion Problems and Materials Requirements for Molten Carbonate Fuel Cells, Proc. Electrochem. Soc., **83-1**, 124-139 (1985).
25. Raymount, M.E.D. Hydrocarbon Processing, 139-142, July 1975.
26. Kotera, Y. International Journal of Hydrogen Energy, **1**, 219-220 (1976).
27. Fukuda, K.; Doklya, M.; Kameyama, T.; Kotera, Y. Ind. Eng. Chem. Fundam. **17**, 243-248 (1978).
28. Edlund, D.J.; Pledger, W.A. J. Mem. Sci. **77**, 255-264 (1993).

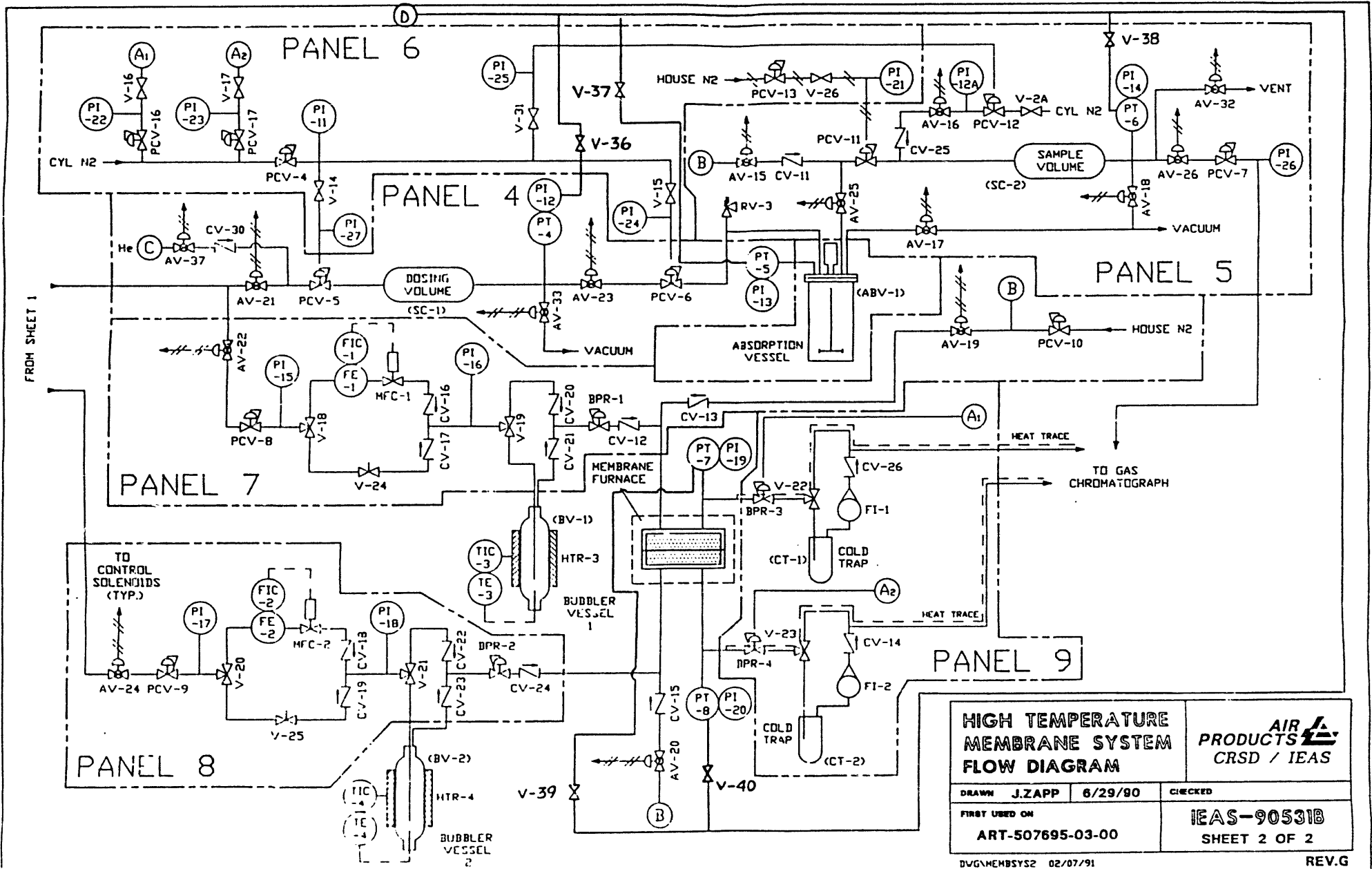
## 7.0 APPENDIX

**7.1 Detailed schematic diagram of absorption and membrane test apparatus and a listing of components.**



<b>HIGH TEMPERATURE MEMBRANE SYSTEM FLOW DIAGRAM</b>	<b>PRODUCTS</b> CRSD / IEAS	
	DRAWN J.ZAPP FIRST USED ON ART-507695-03-00	CHECKED 6/29/90
IEAS-90531B SHEET 1 OF 2		REV.G 02/07/91





<b>HIGH TEMPERATURE MEMBRANE SYSTEM FLOW DIAGRAM</b>		<b>AIR PRODUCTS</b> CRSD / IEAS	
DRAWN	J.ZAPP	6/29/80	CHECKED
FIRST USED ON		IEAS-90531B	
ART-507695-03-00		SHEET 2 OF 2	
DVG\MEMSYS2 02/07/91			REV.G



Materials List for High Pressure High Temperature Membrane and Absorption Unit  
Cell 410

Drawing Designation	Model # Manufacturer	Description	Material of Construction	Pressure Rating (psi)	Temperature Rating (C)
V1, V2, V3, V4, V5, V6, V7, V8, V9, V10, V11, V12, V13, V14, V16, V17, V26, V31	SS-0VS2 Whitey	Integral Bonnet Needle Valve	316 SS	5000	232
V27, V28, V33, V34, V35, V36, V37, V38, V39, V40	SS-0KS2 Whitey	Integral Bonnet Needle Valve	316 SS	5000	93
V15	SS-0RS2 Whitey	Integral Bonnet Needle Valve	316 SS	5000	232
V22, V23	SS-83XF4 Whitey	Valve	SS	1500	232
V18, V19, V20, V21	SS-83XTF4 Whitey	3-way valve	316 SS	1500	232
V24, V25	SS-SS2-D-KZ-S Nupro	Metering Valve	316 SS	2000	149
V2A	SS1VF4 Whitey	Valve	SS	5000	232
V29, V30	SS-44S6 Whitey	Ball Valve	SS	2500	65
CV1, CV2, CV3, CV4, CV5, CV6, CV7, CV8, CV9, CV10, CV11, CV12, CV13, CV14, CV15, CV19, CV20, CV21, CV22, CV23, CV24, CV25, CV26, CV29, CV30	SS-2C-10 Nupro	Check Valve	316 SS	3000	121
CV27, CV28	SS-2C-1/3 Nupro	Check Valve	316 SS	3000	121

Drawing Designation	Model # Manufacturer	Description	Material of Construction	Pressure Rating (psi)	Temperature Rating (C)
AV1, AV2, AV3, AV4, AV5, AV6, AV7, AV8, AV9, AV10, AV11, AV12, AV13, AV14, AV15, AV16, AV17, AV18, AV19, AV20, AV30, AV31, AV32, AV33, AV34, AV35, AV36, AV37	SS-41S2-31C Whitey	Ball Valve	316 SS	2500	65
AV21, AV22, AV23, AV24, AV25, AV26, AV27, AV28, AV29	SS-33VF4-31C Whitey	Ball Valve	316 SS	6000	232
PCV-3	26-1016-24-002 Tescom	Regulator	SS	10000	74
PCV4, PCV12, PCV16, PCV17	44-1114-24 Tescom	Regulator	SS	10000	75
PCV7, PCV10	102-601 GO	Regulator	SS	3000	90
PCV5, PCV6, PCV11, PCV12,	11486P2A Grove	Dome Loaded Regulator	SS	5000	74
PCV13	1Z838D Speedaire	Regulator		250	80
PCV8, PCV9	101-063 GO	Regulator	SS	6000	175
PCV14, PCV15	E11-E-E444 APCI	Regulator	SS	10000	75
SC1	304L-HDF4-500 Whitey	Sample Cylinder	304 SS	1800	N/A
SC2	304L-HDF4-150 Whitey	Sample Cylinder	304 SS	1800	N/A
CT1, CT2	APCI	Water Trap	SS	N/A	N/A
ABV1	Parr HP/HT Custom	Absorption Vessel	Incoloy 800HT	800 WP	800
MV1, MV2	APCI Manuf.	Mix Vessel	304SS	2200	150

Drawing Designation	Model # Manufacturer	Description	Material of Construction	Pressure Rating (psi)	Temperature Rating (C)
RV1, RV2	SS-4R3A Nupro	Relief Valve 2200 psi SP	SS	6000	121
RV3	SS-4R3A Nupro	Relief Valve 900 psi SP	316 SS	6000	121
BPR1, BPR2	101-181 GO	Back- pressure regulator	SS	3000	175
BPR3, BPR4	BPR21U22542 Circle Seal	Back- pressure regulator	SS	6000	200
FI1, FI2	APCI 150mm	Rotameter	SS/Glass	200	120
PT1, PT2, PT3, PT4, PT5, PT6, PT7, PT8	1151GP-8-E-22 Rosemont	Pressure Transducer	SS	6000	71
FCV3	EVA-1XA1-6A Badger Meter	Research Control Valve	SS	5000	65
MFC1, MFC2	201 Porter	Mass Flow Controller	SS	1000	70
PI21, PI26	McDaniel Gauge 0-100 psi	Gauge	SS	300	100
PI12, PI12A	McDaniel Gauge 0-600 psi	Gauge	SS	1800	100
PI6, PI8, PI15, PI16, PI17, PI18	McDaniel Gauge 0-1500 psi	Gauge	SS	4500	100
PI22, PI23, PI24, PI25, PI27	McDaniel Gauge 0-800 pis	Gauge	SS	2400	100
PI1, PI2, PI3	McDaniel Gauge 0-5000 pis	Gauge	SS	15000	100
PI4, PI5	McDaniel Gauge 0-3000 pis	Gauge	SS	9000	100
PI22, PI23, PI24, PI25, PI27	McDaniel Gauge 0-800 pis	Gauge	SS	2400	100
PI7, PI9	McDaniel Gauge 0-300 pis	Gauge	SS	900	100

Drawing Designation	Model # Manufacturer	Description	Material of Construction	Pressure Rating (psi)	Temperature Rating (C)
PI11	Model K 0-3000 psi Gauge	Gauge	SS	9000	100
TIC1, TIC2, TIC3, TIC4	UT-30 Yokogawa	Controller	N/A	N/A	N/A
PIC1	UT-30 Yokogawa	Controller	N/A	N/A	N/A
PI14, PI19, PI20	Red Lion	Digital Panel Meter	N/A	N/A	N/A
TE1, TE2, TE3, TE4		Thermo- couple	316 SS	N/A	850
V41, V42	SS-43S4 Whitey	Ball Valve	316 SS	3000	65

## **7.2 Information relating to the gas chromatograph used in absorption and membrane experiments**

SUPPLEMENTAL INFORMATION FOR ARNEL JOB NO. 1245

GC Operational Parameters

Method #1: Analysis of H<sub>2</sub>, O<sub>2</sub>, N<sub>2</sub>, CO, CH<sub>4</sub>, CO<sub>2</sub>, H<sub>2</sub>S, and COS

Temperatures:

Injection Port A:	120°C
Injection Port B:	120°C
Detector A:	200°C
Detector B:	200°C
Aux. Temp (Valve Oven):	100°C
Oven Maximum:	150°C

Temperature Program:

Initial Oven Temp:	80°C
Initial Time:	25
Rate:	0
Final Temp:	80°C

Detector Signal:

Detector A:	Low Sens,	(+)
Time:	N/A	
Detector B:	Low Sens,	(-)
Time:	N/A	
Signal 1:	A	
Range:	0	
Attn:	0	
Zero:	2.8	
Signal 2:	B	
Range:	0	
Attn:	0	
Zero:	11.0	

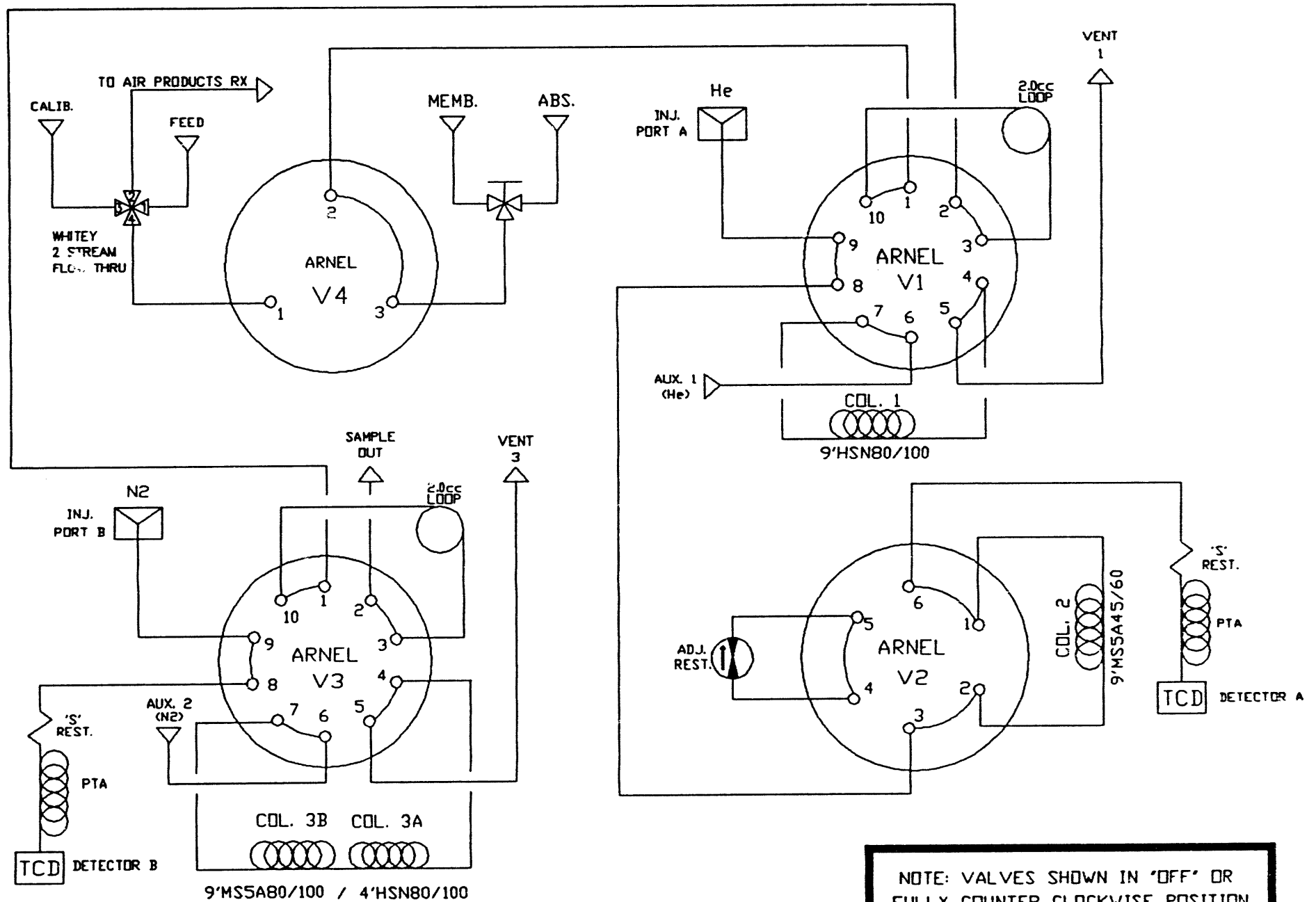


**SUPPLEMENTAL INFORMATION FOR ARNEL JOB NO. 1245**

**Method #1:** Analysis of H<sub>2</sub>, O<sub>2</sub>, N<sub>2</sub>, CO, CH<sub>4</sub>, CO<sub>2</sub>, H<sub>2</sub>S, and COS

**Flows & Pressures: GC Ready at Injection Temperature**

Injection Port A	Packed (He)
Pressure	45 psi
Carrier Flow	30 ml/min. @ Det A
Injection Port B	Packed N <sub>2</sub>
Pressure	41 psi
Carrier Flow	30 ml/min. @ Det B
Aux. 1	40 psi He
Flow	35 ml/min. @ BF vent #1
Aux. 2	48 psi N <sub>2</sub>
Flow	30 ml/min. @ BF vent #3
Detector A	TCD He
Reference	40 ml/min. @ TCD A
Total & Carrier	70 ml/min. @ TCD A
Detector B	TCD N <sub>2</sub>
Reference	40 ml/min. @ TCD B
Total & Carrier	70 ml/min. @ TCD B



AIR PRODUCTS & CHEMICALS, ARNEL JOB 1245

ARNEL ARNEL INCORPORATED

DESIGNER	UPDATED BY: /DATE	FILE NAME	DATE	DRAFTSMAN
REF	T.J.M:5/30/91	1245	4/18/91	THOMAS MASTERHOUSE

SUPPLEMENTAL INFORMATION FOR ARNEL JOB NO. 1245

APPENDIX A

Column Temperature Limits:

Molecular Sieve - 350°C  
Hayesep N - 165°C

COLUMN INFORMATION

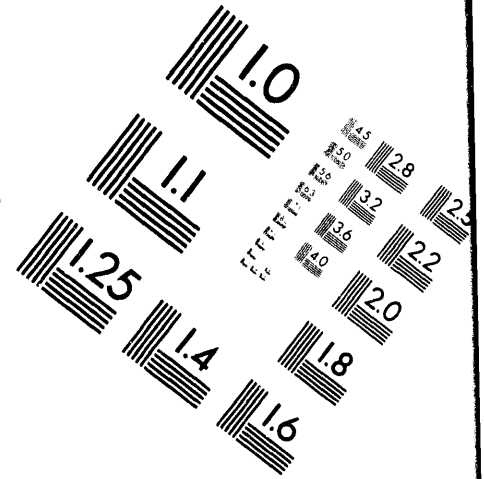
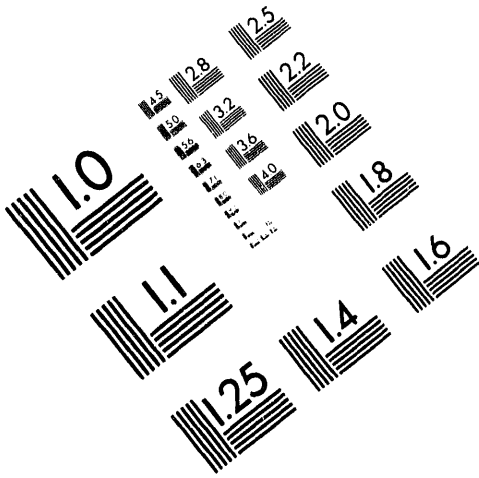
<u>Column No.</u>	<u>Length</u>	<u>Description</u>
1	9'	Hayesep N 80/100
2	9'	Molecular Sieve 5A 45/60
3A	4'	Hayesep N 80/100
3B	9'	Molecular Sieve 5A 80/100
PTA's	3'	Chromosorb P aw 60/80



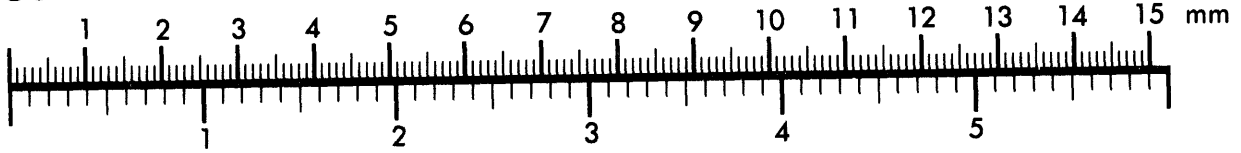
**AIM**

**Association for Information and Image Management**

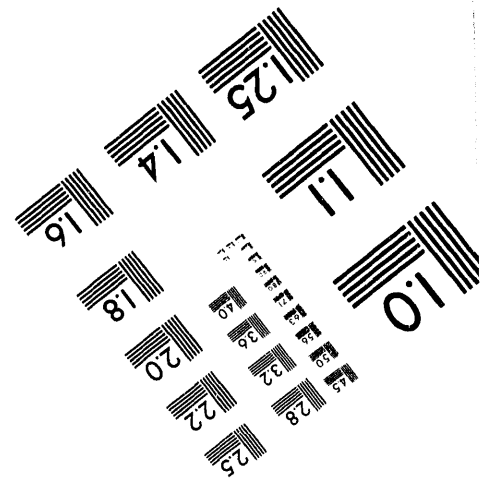
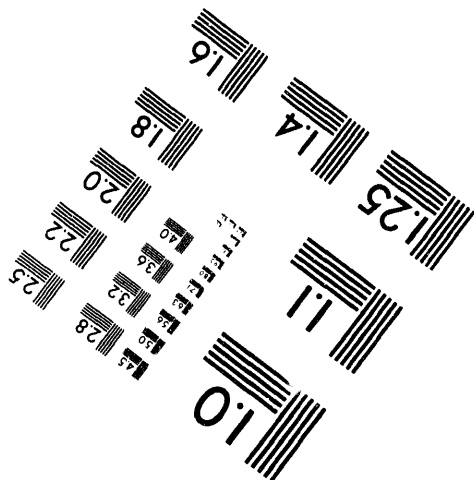
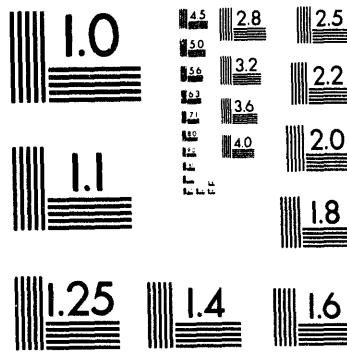
1100 Wayne Avenue, Suite 1100  
Silver Spring, Maryland 20910  
301/587-8202



Centimeter



Inches



MANUFACTURED TO AIM STANDARDS  
BY APPLIED IMAGE, INC.

**2 of 3**

### **7.3 Research Triangle Institute Final Report**

**DEVELOPMENT OF FACILITATED TRANSPORT CERAMIC  
MEMBRANES — EXPERIMENTAL TESTING**

**FINAL REPORT**

**Work performed under a subcontract with  
prime contract No.: DE-AC21-89MC26038**

**Prepared by**

**A.S. Damle  
S.K. Gangwal  
Research Triangle Institute  
P.O. Box 12194  
Research Triangle Park, NC 27709-2194**

**Prepared for**

**Air Products and Chemicals, Inc.  
7201 Hamilton Boulevard  
Allentown, PA 18195-1501**

**January 1994**

**DEVELOPMENT OF FACILITATED TRANSPORT CERAMIC  
MEMBRANES — EXPERIMENTAL TESTING**

**FINAL REPORT**

**Work performed under a subcontract with  
prime contract No.: DE-AC21-89MC26038**

**Prepared by**

**A.S. Damle  
S.K. Gangwal  
Research Triangle Institute  
P.O. Box 12194  
Research Triangle Park, NC 27709-2194**

**Prepared for**

**Air Products and Chemicals, Inc.  
7201 Hamilton Boulevard  
Allentown, PA 18195-1501**

**January 1994**



## Table of Contents

Section		Page
	List of Figures .....	iv
	List of Tables .....	vi
	Executive Summary .....	vii
1	Introduction .....	1
1.1	Facilitated Transport Process Concept/Chemistry .....	1
2	Experimental .....	4
2.1	Experimental System .....	4
2.1.1	Preliminary Disk Membrane Apparatus .....	4
2.1.2	Continuous Long-term Disk Membrane Test Apparatus .....	5
2.1.3	Continuous Long-term Tubular Membrane Test Apparatus .....	9
2.1.4	Simulated Coal Gas and Sweep Gas Compositions .....	9
2.1.5	Experimental Procedure .....	11
2.2	Experimental Matrix .....	11
3	Results and Discussion .....	13
3.1	Preliminary Disc Membrane Testing .....	13
3.1.1	Run No. 1 .....	13
3.1.2	Run No. 2 .....	16
3.1.3	Run No. 4 .....	17
3.1.4	Run No. 5 .....	17
3.1.5	Summary and Discussion .....	17
3.2	Continuous Long-term Disc Membrane Testing .....	19
3.2.1	Run No. 6 .....	19
3.2.2	Run No. 7 .....	25
3.2.3	Run No. 8 .....	25
3.2.4	Run No. 9 .....	26
3.2.5	Run No. 10 .....	26
3.2.6	Run No. 11 .....	28
3.2.7	Run No. 12 .....	28
3.2.8	Run No. 13 .....	29
3.2.9	Run No. 14 .....	29
3.2.10	Summary and Discussion .....	29
3.3	Continuous Long-term Tubular Membrane Testing .....	37
3.3.1	Run No. T-2 .....	37
3.3.2	Run No. T-3 .....	39
3.3.3	Run No. T-4 .....	44
3.3.4	Run No. T-5 .....	44
3.3.5	Summary and Discussion .....	51

## Table of Contents (con.)

Section		Page
4	Theoretical Modeling of Facilitated Transport .....	52
4.1	Analysis of Steady-state Data .....	52
4.2	Estimation of $K$ and $D_{s..}$ from Steady-state Experimental Permeation Data .....	55
4.2.1	Data from Run No. 6 .....	55
4.2.2	Data from Run No. 14 .....	57
4.3	Analysis of Transient Data .....	58
4.3.1	Estimation of Diffusion Coefficient from Experimental Data .....	60
4.4	Maximum Achievable $H_2S$ Concentration in Permeate .....	62
5	Process Evaluation .....	65
5.1	Estimation of Membrane Module Size for a 100-MW IGCC Plant ...	66
6	Conclusions and Recommendations .....	67
7	References .....	69

## List of Figures

Number		Page
1-1	Cross-sectional view of the active molten salt film in an IMS membrane for the separation of H <sub>2</sub> S. ....	3
2-1	Test apparatus used in preliminary disc membrane studies .....	6
2-2	Schematic drawing of membrane test cell design .....	7
2-3	Schematic of a continuous condensate drain system .....	8
2-4	Schematic of a symmetrical half of the tubular membrane reactor assembly .....	10
3-1	Helium and H <sub>2</sub> S concentration with time (Run #6, 5/3/93, 50 psig, 556 °C) .....	21
3-2	Helium, hydrogen, and H <sub>2</sub> S concentrations with time (Run #6, 5/4/93, 50 psig, 556 °C) .....	22
3-3	Helium, hydrogen, and H <sub>2</sub> S concentrations with time (Run #6, 5/5/93, 50 psig, 556 °C) .....	23
3-4	Helium, hydrogen, and H <sub>2</sub> S concentrations with time (Run #8, 6/4-6/6/93, 50 psig, 615 °C) .....	24
3-5	Helium, hydrogen, and H <sub>2</sub> S concentrations with time (Run #9, 6/23/93, 50 psig, 600 °C) .....	27
3-6	H <sub>2</sub> S, helium, and hydrogen concentrations with time (Run #14, 8/30-9/1/93, 50, 100, 200 psig, 560 °C) .....	30
3-7	H <sub>2</sub> S, helium, and hydrogen concentrations with time (Run #14, 9/1-9/4/93, 50, 100, 200 psig, 560 °C) .....	31
3-8	Cross section of an unused thicker membrane .....	33
3-9	Cross section of a membrane used in Run No. 10 .....	34
3-10	Cross section of a membrane used in Run No. 6 .....	35
3-11	Cross section of a membrane used in Run No. 8 .....	36
3-12	H <sub>2</sub> S concentration with time (Run #T-2, 11/17-11/22/93, 50, 100 psig, 500-560 °C) .....	40

## List of Figures (con.)

Number		Page
3-13	Helium and hydrogen concentration with time (Run #T-2, 11/17-11/22/93, 50, 100 psig, 500-560 °C) . . . . .	41
3-14	H <sub>2</sub> S/He selectivity with time (Run #T-2, 11/17-11/22/93, 50, 100 psig, 500-560 °C) . . . . .	42
3-15	Used tubular membrane showing downward salt movement . . . . .	43
3-16	H <sub>2</sub> S concentration with time (Run #T-4, 12/15-12/22/93, 50 psig, 510-520 °C) . . . . .	45
3-17	Helium and hydrogen concentration with time (Run #T-4, 12/15-12/22/93, 50 psig, 510-520°C). . . . .	46
3-18	H <sub>2</sub> S/He and H <sub>2</sub> /He with time (Run #T-4, 12/15-12/22/93, 50 psig, 510-520 °C) . . . . .	47
3-19	H <sub>2</sub> S concentration with time (Run #T-5, 12/27-12/31/93, 50 psig, 515 °C) . . . . .	48
3-20	Helium and hydrogen concentration with time (Run #T-5, 12/27-12/31/93, 50 psig, 515 °C) . . . . .	49
3-21	H <sub>2</sub> S/He and H <sub>2</sub> /He selectivities with time (Run #T-5, 12/27-12/31/93, 50 psig, 515 °C) . . . . .	50
4-1	Schematic of concentration gradients in the molten salt . . . . .	54
4-2	Variation of flux rate with time—diffusion through a plane sheet . . . . .	61

## List of Tables

Number		Page
3-1	Percent Salt Infiltrations in the Membranes Used . . . . .	14
3-2	Experimental Results of Preliminary Disc Membrane Experiments . . . . .	15
3-3	Experimental Results of Continuous Long-term Disc Membrane Experiments . . . . .	20
3-4	Experimental Results of Continuous Long-term Tabular Membrane Experiments . . . . .	38

## EXECUTIVE SUMMARY

The economic viability of advanced power generation concepts such as Integrated Gasification Combined Cycle (IGCC) and Direct Coal-Fired Turbines (DCFT) technologies depends on efficient removal of contaminants at the high temperature-high pressure (HTHP) operating conditions. Molten salt impregnated ceramic membranes provide a novel potential technique for removal of contaminant gases such as  $H_2S$ ,  $NH_3$ ,  $SO_2$  and  $NO_x$  based on facilitated transport mechanism for the contaminant species. In recent years, microporous ceramic membranes have been investigated for gas separation applications based upon passive mechanisms such as Knudson diffusion and molecular sieving. However, such passive separations cannot remove low concentration contaminants efficiently. Facilitated transport mechanism allows selective removal of such contaminants based on their chemical reactivity toward suitable reagents.

In this project, the technical feasibility of molten salt impregnated ceramic membranes, provided by Air Products and Chemicals, Inc., was investigated experimentally for removal of  $H_2S$  from coal gas at HTHP conditions. Both the disc and tubular membrane geometries were investigated, although the bulk of the membrane testing was conducted with membrane discs. Alkali carbonate salts were impregnated in microporous aluminum nitride discs/tubes to prepare these membranes. The microporous substrates were fabricated by Golden Technologies, Inc., and were infiltrated with molten salts by Air Products and Chemicals, Inc.

The experimental testing of membranes was conducted in three distinct phases. In the first phase, preliminary short-term experiments were conducted with disc membranes to verify enhanced transport of  $H_2S$ . These experiments determined experimental conditions under which measurable  $H_2S$  permeation rates could be obtained, and established the facilitated transport mode for  $H_2S$  permeation. These experiments, conducted at temperatures of 560 to 600 °C and pressures of 50 to 200 psig, also identified a need for a long-term stable operation to obtain steady-state permeation data. During this first phase, permeation data were obtained from a total of four membranes.

The experimental system used during the preliminary experiments was successfully modified to allow long-term, continuous, unattended testing of membranes. During the second phase long-term experiments were conducted using a total of nine disc membranes. These experiments confirmed the enhanced transport of  $H_2S$  with  $H_2S$  permeabilities in the range of 13,000 to 200,000 Barrers and  $H_2S$  to helium selectivities as high as 18. These membranes also indicated high permeabilities for hydrogen and helium indicating substantial leakage flow across a membrane. Similar to the first phase, the second phase studies were also conducted at 560 to 600 °C and 50 to 200 psig pressure. The results obtained with these membranes were inconsistent with some membranes not showing any  $H_2S$  permeation at all. The inconsistencies in the performance of different membranes are thought to be due to nonuniform or incomplete salt infiltration in the ceramic porous matrix. For the membranes showing enhanced  $H_2S$  transport, long periods of time, of the order of several hours, were needed to achieve steady-state permeation conditions indicating slow liquid phase diffusion process.

The long-term disc membrane tests indicated several key trends expected with facilitated transport: (1) lower permeabilities at higher pressures, (2) greater permeabilities at higher temperatures, (3) gradual increase in  $H_2S$  permeation across membrane, and (4)  $>1$  selectivity

for species permeated by facilitated transport. All of the above trends were observed in spite of substantial porous leakage flow.

The observed H<sub>2</sub>S selectivities in the long-term disc membrane testing were strongly affected by large leakage flow of helium and hydrogen. To increase the membrane surface area and to reduce overall contribution by leakage at seals, long-term experiments were conducted using three tubular membranes during the third phase of the experimental program. Testing at a temperature of 560 °C, typically used for disc membrane studies, indicated rapid increase in leakage flow with time indicating downward movement of salt within the ceramic matrix due to gravity. Further testing indicated that the membrane temperature can be increased only 10 to 20 °C above salt melting point without a quick increase in leakage flow. The lower operating temperature coupled with a greater thickness as compared to disc membranes resulted in significantly lower H<sub>2</sub>S permeabilities with tubular membranes. The time required for steady-state operation was also found to be considerably longer with tubular membranes as steady state was not observed even after several days of operation.

Theoretical analysis of the facilitated transport process indicated that uphill transport of H<sub>2</sub>S is possible, and that up to 13 percent H<sub>2</sub>S permeate stream could be obtained, with 0.5 percent H<sub>2</sub>S coal gas, without any transmembrane pressure differential. However, the above analysis assumed no mass transfer resistance. The membrane studies indicated a slow liquid phase diffusion process. For practical application of this concept, the observed H<sub>2</sub>S flux rates need to be increased by an order of magnitude and the time requirement to achieve steady-state operation needs to be reduced by two orders of magnitude. The salt retention in the porous matrix is essential for this concept to work. Thus, the mean pore size of the ceramic matrix needs to be reduced with elimination of large pores >1 μm to improve the ability of the ceramic matrix to hold molten salt in place by capillary suction.

## SECTION 1

### INTRODUCTION

The successful development of advanced power generation systems such as Integrated Gasification Combined Cycle (IGCC) and Direct Coal Fired Turbines (DCFT) technologies depends on an economically viable and environmentally acceptable removal of contaminant gases. Facilitated transport membranes that can operate under the high-temperature, high-pressure (HTHP) conditions within these processes offer a potential technique for removal of contaminant gases such as  $H_2S$ ,  $NH_3$ ,  $SO_2$ , and  $NO_x$ . In recent years, microporous ceramic membranes have been investigated for gas separation applications based on Knudsen diffusion and molecular sieving mechanisms. However, such passive separations will not be able to remove low concentration contaminants. Facilitated transport mechanism offers a novel technique for selective removal of such contaminants based on their reactivity toward suitable reagents. In this project, the technical feasibility of molten salt impregnated ceramic membranes, developed by Air Products and Chemicals, Inc., was experimentally investigated for removal of  $H_2S$  from coal gas.

Both the disc and tubular membrane geometries were investigated, although the bulk of the membrane testing was conducted with the membrane discs. Alkali carbonate salts were impregnated in microporous aluminum nitride discs/tubes to prepare these membranes. The aluminum nitride microporous disc and tubular membrane substrates were fabricated by Golden Technologies, Inc., and were infiltrated with molten carbonate salt by Air Products & Chemicals, Inc. Permeation rates of  $H_2S$  along with other gas species across the membrane were measured under different operating conditions to determine the effectiveness of these membranes for separating  $H_2S$  from coal gas. Experiments were conducted over a period of 1 year from October 1992 through December 1993. A brief description of the facilitated transport concept and process chemistry involved is given below.

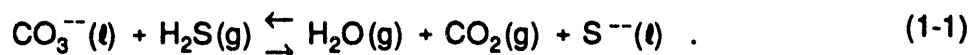
The experimental systems used are described in Section 2 and the experimental results are discussed in Section 3. Section 4 provides theoretical estimation of important parameters governing facilitated transport of  $H_2S$  and Section 5 provides a brief process evaluation.

#### 1.1 FACILITATED TRANSPORT PROCESS CONCEPT/CHEMISTRY

In the facilitated transport concept, an active reagent, capable of reacting reversibly with the desired contaminant, is incorporated in the pores of a microporous membrane. This concept combines the absorption/reaction of the contaminant species in the reagent and subsequent stripping of the contaminant species with regeneration of the reagent, in one unit. A number of alkali metal carbonates are liquids in the range of 400 and 900 °C and are capable of reacting reversibly with  $H_2S$  and thus are excellent candidates for the facilitated separation of  $H_2S$  from coal gas under HTHP conditions. The reaction of carbonate melts with  $H_2S$  in the presence of  $H_2O$  and  $CO_2$  has been studied by several investigators (Moore, et al., 1980; Stegen, 1982; and Lyke et al., 1985a, 1985b) to develop a hot gas cleanup system for IGCC/molten carbonate fuel cell power plants.

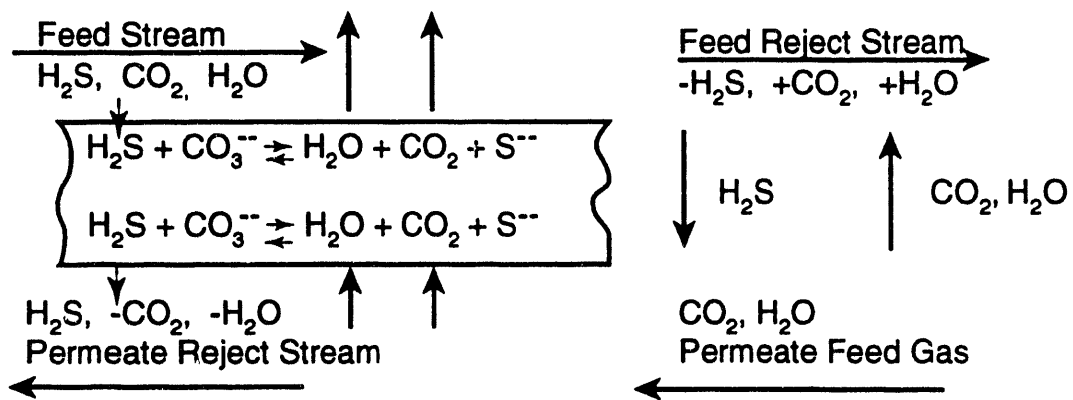


Figure 1-1 illustrates the process chemistry involved in the H<sub>2</sub>S removal from coal gas by the molten carbonate salt impregnated in a microporous membrane. The membrane is exposed on the feed side to a high-pressure coal gas stream predominantly containing H<sub>2</sub>, CO, CO<sub>2</sub>, H<sub>2</sub>O, CH<sub>4</sub>, and H<sub>2</sub>S, while the permeate side membrane/gas interface is swept by a gas mixture containing CO<sub>2</sub> and H<sub>2</sub>O. At the feed membrane/gas interface, H<sub>2</sub>S reacts with the alkali carbonate melt to produce water, carbon dioxide, and alkali sulfide:



Since free H<sub>2</sub>O and CO<sub>2</sub> have a very low physical solubility in the molten salt, they will be largely liberated into the gas phase and go into the feed reject stream. Sulfide ions, the major product remaining in the melt, will diffuse to the permeate membrane/gas interface where it will react with the CO<sub>2</sub> and H<sub>2</sub>O in the sweep gas stream by the same reversible reaction (1-1) to form H<sub>2</sub>S and regenerate carbonate salt (CO<sub>3</sub><sup>--</sup>). The hydrogen sulfide is liberated into the permeate stream, and with back diffusion of CO<sub>3</sub><sup>--</sup> ions to the feed side the overall transport cycle is completed.

This overall cycle amounts to a carrier-mediated transport of H<sub>2</sub>S from the feed to permeate, coupled with a flow of steam and CO<sub>2</sub> in the opposite direction (i.e., from permeate to feed). According to the stoichiometry of Equation (1-1), for each mole of H<sub>2</sub>S that is removed from the IGCC hot-gas stream, 1 mol of H<sub>2</sub>O and CO<sub>2</sub> is introduced. Because of the coupled nature of this transport process, the H<sub>2</sub>S flux is determined by the partial pressure gradients of all three permeating gases (H<sub>2</sub>S, CO<sub>2</sub>, and H<sub>2</sub>O) across the membrane. Thus, it would be possible to transport H<sub>2</sub>S across the membrane against its own concentration gradient, i.e., uphill transport, by setting appropriate gradients for the other two species. Such uphill transport would also allow near-complete removal of H<sub>2</sub>S from coal gas. Since the transport of H<sub>2</sub>S depends on its reaction, a highly selective separation of H<sub>2</sub>S from coal gas can be achieved.



The mechanism of transport of  $\text{H}_2\text{S}$ , with a coupled transport of  $\text{H}_2\text{O}$  and  $\text{CO}_2$  in the reverse direction is indicated.

Figure 1-1. Cross-sectional view of the active molten salt film in an IMS membrane for the separation of  $\text{H}_2\text{S}$ .

## SECTION 2

### EXPERIMENTAL

The experimental testing of the membranes supplied by Air Products and Chemicals, Inc., was conducted in three distinct phases. In the first phase preliminary short-term experiments were conducted with disc membranes to determine the experimental conditions under which measurable H<sub>2</sub>S permeation rates could be obtained. These runs also provided an indication of permeation of other gas species, system stability, time requirement for achieving a steady state, and requirements for gas chromatographs (GCs) for adequate analytical resolution. During these experiments, a set of operating conditions was held constant for periods of only 1 to 4 hours. A total of four membranes were tested in this phase. The disc membranes were approximately 1 in. dia and 0.1 in. thick. The mean pore size was estimated to be <1 μm. The percent by weight of salt infiltration in these four membranes was estimated to be from 72 to 82 percent.

In the second phase, disc membranes were tested in continuous long-term experiments to determine permeation of H<sub>2</sub>S and other species over a long period of time as a function of operating conditions. A total of nine membranes were used in this phase, with the test durations for different membranes ranging from a period of one to several days. Seven of these membranes were similar to the ones used in the preliminary experiments, i.e., approximately 1 in. dia, and 0.1 in. thick. One disc membrane tested was slightly thicker, about 0.12 in. thick and one membrane was thinner with 0.06 in. thick. The mean pore size was again estimated to be <1 μm. The percent by weight of salt infiltration in these membranes was estimated to be from 65 to 74 percent except for the one thicker membrane for which the percent salt infiltration was estimated to be only 34 percent.

In the third phase, tubular membranes were tested in continuous long-term experiments to determine the permeation characteristics as a function of operating conditions. A total of three tubular membranes were used in this phase, with the test durations for these membranes ranging over several days. The mean pore size of the tubular membranes was also expected to be <1 μm. The tubes were approximately 15-mm OD, 8-mm ID, and 3.5-mm thick. The percent of salt infiltration in the tubular membranes was estimated to be from 74 to 82 percent by weight. The ceramic tubes ranged from 8 in. to 10 in. in length.

#### 2.1 EXPERIMENTAL SYSTEM

Experimental systems used during the three testing phases were slightly different and are described below. The simulated coal gas and sweep gas compositions as well as experimental procedures are also outlined below.

##### 2.1.1 Preliminary Disc Membrane Test Apparatus

The HTHP disc membrane testing facility used in the preliminary studies is shown schematically in Figure 2-1. The gas delivery system can supply the simulated coal gas composition or an inert 5 percent CO<sub>2</sub> in N<sub>2</sub> purge gas to the feed side of the membrane as well as a 30 percent CO<sub>2</sub> in N<sub>2</sub> sweep gas composition to the permeate side of the membrane. The flow rate of the gases is controlled by calibrated mass flow controllers (MFCs). The water vapor required for both the feed and sweep gases is generated by high pressure positive displacement

pumps and heating tapes wrapped around the stainless steel supply tubings. The water vapors are mixed with the preheated feed and sweep gases prior to introduction in the membrane test cell. The membrane is housed in a stainless steel holder which is maintained at a controlled temperature in a tubular furnace. The exit feed and sweep gas streams are cooled in condensers to remove water vapor and then combined before they exit through a dryer, filter, and a back pressure regulator (BPR). The single BPR controls the pressure on both sides of the membrane with a minimal transmembrane pressure drop. The pressure drop across the membrane is monitored by a differential pressure gauge. The transmembrane pressure drop can be adjusted to a small extent by changing the ratio of the feed and sweep gas flow rates. The feed and sweep gas exit streams are analyzed by on-line GCs.

The membrane holder used in these tests was provided by Air Products & Chemicals, Inc., and is shown schematically in Figure 2-2. In the original design a gold-plated metal "C" ring was used to seal the membrane against the holder. However, this sealing method led to frequent cracking of the membranes during loading. Therefore, a graphite tape was wrapped around the circular disc membrane in these preliminary experiments. Part of the tape also extended on the flat portion of the membrane along its periphery which acted as a seal against the membrane holder. This procedure reduced the probability of cracking the membranes. Since the graphite tape covered part of the flat portion of the disc membrane, the effective surface area exposed to feed gas was reduced from 5 to about 2.3 cm<sup>2</sup>.

Because of relatively high water vapor rates used, the condensers needed frequent manual draining to prevent buildup and carryover into the exit gas streams. The positive displacement pumps also required occasional fillups during an experimental run. Because of the limitations imposed by condenser draining and pump fillup requirements, the experiments in this phase could not be run unattended for an extended period of time.

### **2.1.2 Continuous Long-term Disc Membrane Test Apparatus**

In the second phase of the membrane testing, the system used in the preliminary studies was modified to allow for continuous long-term unattended operation. Helium was substituted for a part of inert nitrogen in the coal gas to provide an unambiguous quantitative detection of leak flow through unfilled membrane pores or around the graphite seal. Annular graphite gaskets were used for sealing the membrane instead of wrapping a graphite tape around the membrane. In addition, GCs with higher resolution detectors were used to provide simultaneous measurements of H<sub>2</sub>S, He, and H<sub>2</sub> in the permeate stream.

To allow for continuous long-term unattended operation, a modified condensate drain system was installed on both the feed and sweep side condensers. The drain system is shown schematically in Figure 2-3. A small continuous gas flow is maintained through the drain system to force the accumulated condensate in a large reservoir continuously. Tests indicated that these systems could be operated successfully with as little as 200 cc/min vent gas flow rate.

The positive displacement pumps were replaced by high-pressure liquid pumps which could withdraw water continuously from a large reservoir increasing its capacity substantially. A flow control valve was installed in the sweep gas exit line prior to its merging with the feed gas exit stream. This valve allowed adjustment of the transmembrane differential pressure drop without changing the feed and sweep gas flow rates. Two cylinder manifolds were installed for both the feed gas and sweep gas continuous supply. Each manifold is connected to two gas cylinders of the same composition, which allows replacing an empty cylinder without interrupting system flows.

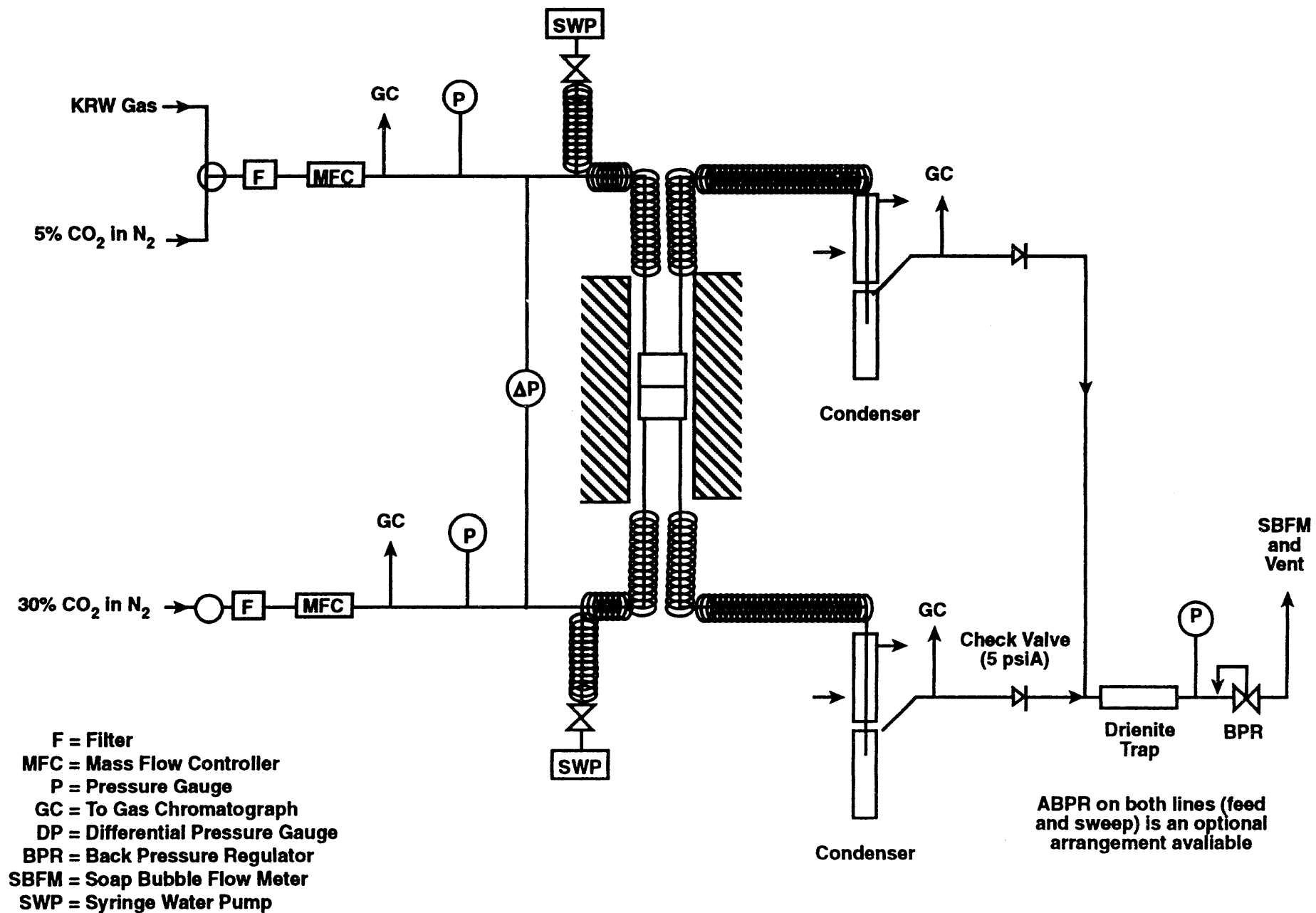
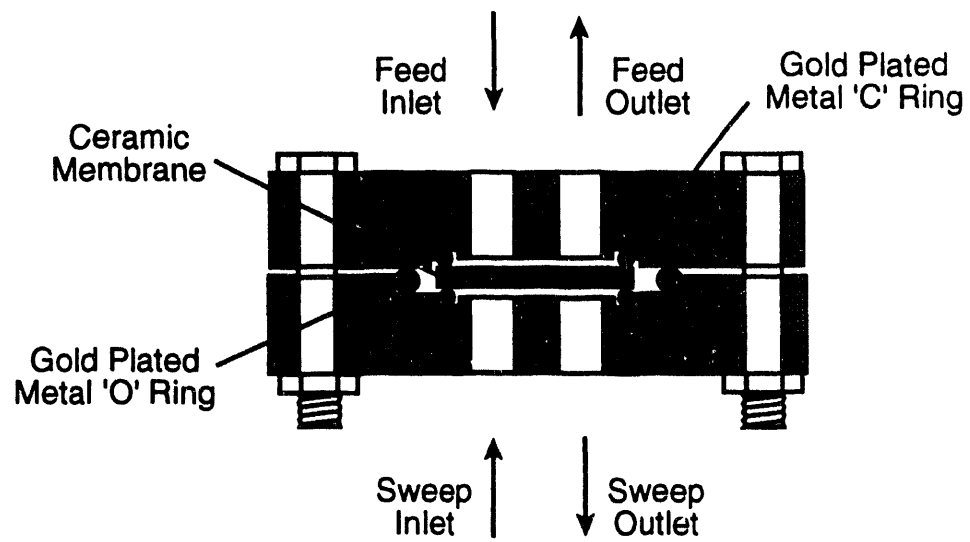
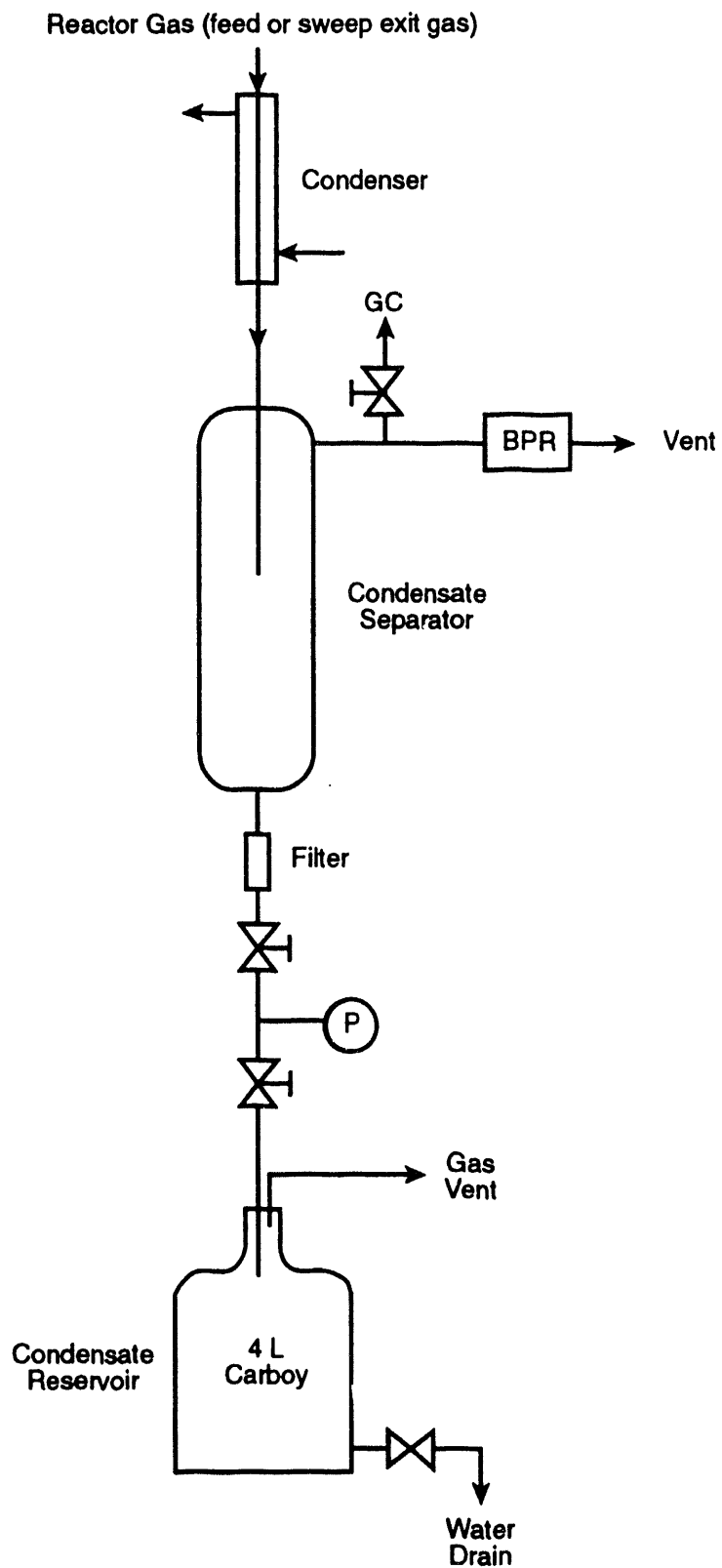


Figure 2-1. Test apparatus used in preliminary disc membrane studies.



**Figure 2-2. Schematic of membrane test cell design.**



**Figure 2-3. Schematic of a continuous condensate drain system.**

### 2.1.3 Continuous Long-term Tubular Membrane Test Apparatus

For testing the tubular membranes, the membrane disc holder was replaced by a 1.5-in. dia, 18-in. long stainless-steel reactor tube closed by 1.5 in. caps. Weld fitting joints were used to allow for feed and sweep inlet and outlet connections. The ceramic membrane tubes were approximately 15 mm in outside diameter. A tube was connected to 1/4 in. stainless-steel tubing using 15 mm to 1/2 in. and 1/2 in. to 1/4 in. stainless-steel reducing unions as shown in the reactor schematic in Figure 2-4. Custom-designed 15-mm graphite ferrules were used for sealing a membrane tube in the reducing unions on both ends. The existing furnace was large enough to house the tubular membrane reactor assembly. All other system components were the same as used in the continuous long-term disc membrane testing.

### 2.1.4 Simulated Coal Gas and Sweep Gas Compositions

For bulk of the experimental runs, gas composition similar to the KRW gasifier coal gas composition was used as the membrane feed gas. KRW coal gas typically consists of 10 percent hydrogen, 15 percent carbon monoxide, 5 percent carbon dioxide, 0.5 percent hydrogen sulfide, 54.5 percent nitrogen, and 15 percent water vapor. Dry gas mixture consisting of 12 percent hydrogen, 18 percent carbon monoxide, 6 percent carbon dioxide, 0.6 percent hydrogen sulfide with balance nitrogen was therefore used as feed gas in the preliminary disc experiments. During these experiments, it became apparent that it would be desirable to include a unique inert gas species in the feed gas to quantitatively determine the contribution of leak to the overall permeation. Six percent helium was therefore substituted for nitrogen as a tracer gas for the long-term disc and tubular membrane experiments. The exact gas composition used in each individual experiment was somewhat different due to the variability in the gas received from suppliers and was noted for all runs. In some experiments, a 2 percent hydrogen sulfide in nitrogen gas mixture was used as a feed gas to maximize  $H_2S$ ,  $CO_2$ , as well as  $H_2O$  concentration gradients for greater facilitation of  $H_2S$  transport.

In all experiments 30 percent  $CO_2$  in  $N_2$  was used as a dry sweep gas. The water vapor concentration in the sweep stream was always kept slightly greater than that in the feed stream. For the preliminary disc membrane experiments and earlier long-term disc membrane experiments, 15 percent water vapor was used in the feed stream as being typical of the KRW coal gas. The water vapor concentration in the sweep gas in these runs was kept about 16 percent. During the earlier long-term membrane experiments it became apparent that carbon deposition may become a problem for longer duration runs. Therefore, in subsequent runs, the water vapor concentration in the feed gas was increased to 25 percent to prevent carbon formation. The water vapor concentration in the sweep gas was kept at 26 percent in these experiments.

During the initial heating of the membrane to the desired temperature, a 5 percent  $CO_2$  in  $N_2$  gas was used as a purge gas instead of actual coal gas. Also, during the preliminary disc membrane experiments, a membrane was often kept molten during nontesting hours while maintaining a small purge gas and sweep gas flows on the two sides of the membrane.



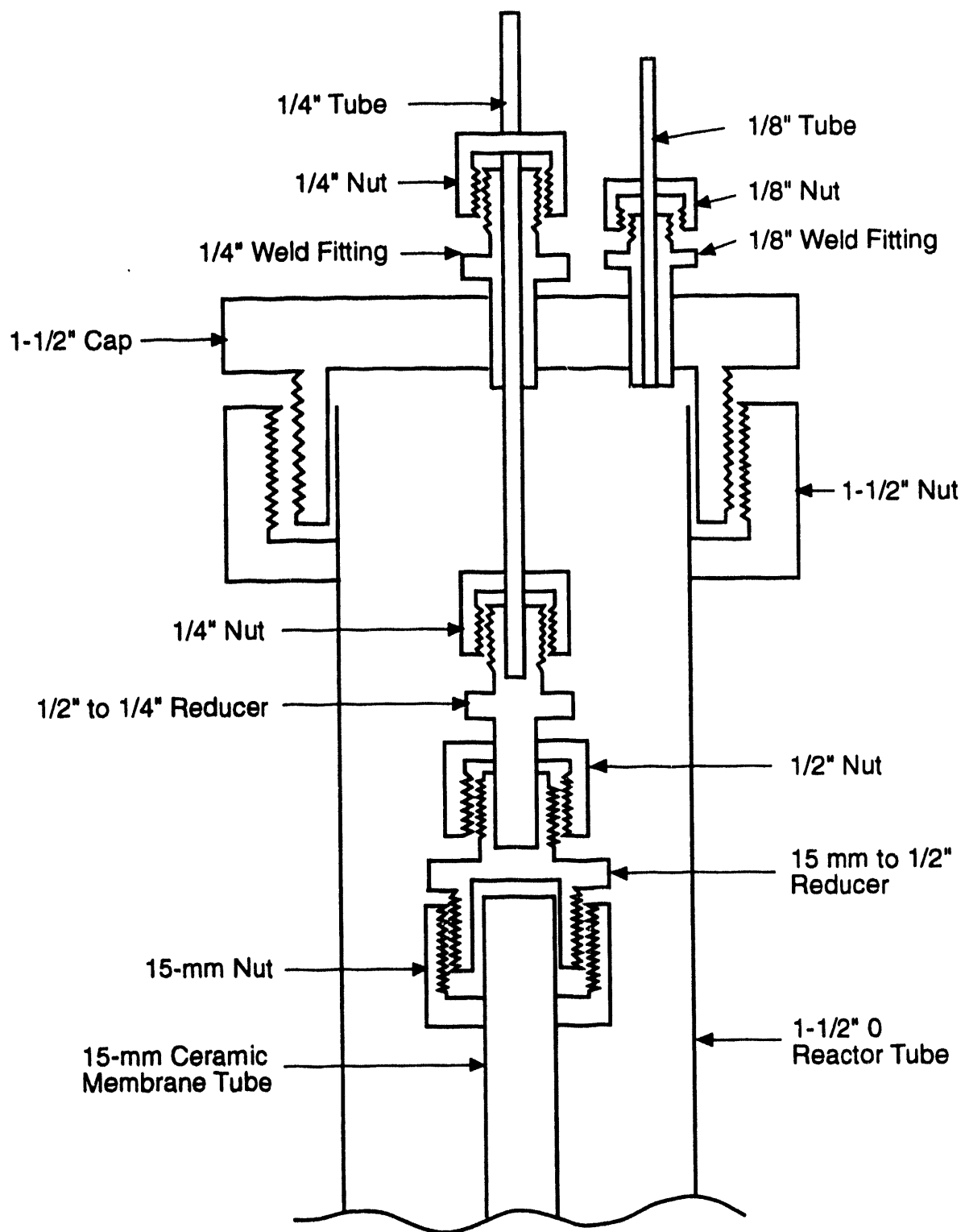


**Figure 2-4. Schematic of a symmetrical half of the tubular membrane reactor assembly.**

### 2.1.5 Experimental Procedure

Generally, the same experimental procedure was used for all runs. A disc or tubular membrane was loaded in a holder or a tubular reactor, respectively, using graphite tape (preliminary disc membrane experiments), annular graphite gaskets (long-term disc membrane experiments), or graphite ferrules (tubular membranes) for sealing the membrane against the housing. The membrane holder is then leak tested at room temperature by pressurizing the feed side with nitrogen and monitoring the leak flow by bubble flow meter. For tubular membranes the membrane tube was pressurized on the inside. The bolts on the holder or the fittings in the tubular membranes were then tightened until the leak rate was minimized at 20 psig feed pressure. For disc membranes it was often possible to stop the leak completely. All tubular membranes, however, were found to be porous enough to permit a very small leak flow of the order of 0.2 to 0.4 cm<sup>3</sup>/min at 20 psig pressure differential. The maximum transmembrane pressure drop imposed in actual runs was about 20 in. of water. Thus, the expected leak rate in the case of tubular membranes was still very small. The leak rate by porous flow in actual experiments was determined from the helium permeation rates during the long-term experiments.

The loaded membrane holder or the tubular reactor is then installed in the furnace and connected to the respective feed and sweep lines. The membrane is then heated gradually, in stages, to the desired temperature while flowing the purge gas on the feed side and the sweep gas on the permeate side at the desired flow rates. Upon reaching the target temperature, the system pressure is raised to the appropriate level. Both the feed and sweep side high pressure water pumps are then turned on to inject the appropriate amount of water vapor. Deionized water was used as the source of water. During the early preliminary disc membrane experiments it became apparent that the dissolved oxygen in the deionized water may be contributing to some extent to the membrane deactivation by oxidizing the alkali salt to sulfates. To eliminate this possibility, the water supply was aerated continuously by nitrogen to remove dissolved oxygen. The transmembrane pressure drop across the membrane was usually adjusted to 10 to 20 in. of water on the sweep side to reduce the viscous flow contribution.

After allowing enough time for the steam to reach condensers, the flow on the feed side was switched from the purge gas to the coal gas. The exit sweep stream was continuously monitored by GCs to determine H<sub>2</sub>S, H<sub>2</sub>, and He concentrations. Since the permeation rates of all species were fairly small, no measurable change in the feed gas composition was anticipated. Therefore, the feed gas exit stream was monitored only periodically with another on-line GC.

## 2.2 EXPERIMENTAL MATRIX

The primary operating variables during testing of a membrane were membrane temperature and system pressure. In bulk of the experiments, KRW coal gas was used as a feed gas. In some experiments, a 2 percent hydrogen sulfide in nitrogen gas mixture was used as a feed gas to maximize H<sub>2</sub>S transport. The membrane temperatures during the disc experiments ranged from 555 to 660 °C and the system pressures ranged from 50 to 200 psig. The bulk of the experiments were conducted at about 560 °C and 50 psig system pressure. During the long-term tubular membrane experiments the membrane temperatures ranged from 490 to 560 °C and the system pressure ranged from 50 to 100 psig. The bulk of the tubular membrane experiments were conducted at 50 psig pressure.

The dry sweep gas flow rate for the preliminary disc membrane experiments ranged from 1.3 to 2 std. L/min, whereas, during the long term continuous experiments approximately 1 std. L/min of dry sweep gas flow rate was used. The dry feed gas flow rate for all experiments was approximately 1 std. L/min.

In all the preliminary disc membrane experiments and in early long-term continuous disc membrane experiments, approximately 15 percent water vapor was used on the feed side as being typical of the KRW coal gas. In the latter part of the long-term disc membrane experiments and in all of the tubular membrane experiments, the feed side water vapor content was increased to 25 percent to minimize carbon deposition. The corresponding sweep side water vapor contents were 16 and 26 percent, respectively.

## SECTION 3

### RESULTS AND DISCUSSION

Permeation data collected in all three experimental phases were analyzed to determine the membrane permeability for  $H_2S$  as well as other gases and the membrane selectivity with respect to  $H_2S$  as a function of operating conditions. Since the experimental setups were somewhat different in the three phases of the membrane testing the results obtained in each phase are discussed separately. The membranes used in all of the experiments and their respective percent salt infiltrations are given in Table 3-1.

#### 3.1 PRELIMINARY DISC MEMBRANE TESTING

The objective of the preliminary disc membrane experiments was to verify the transport of  $H_2S$  across the molten salt impregnated ceramic membranes and to determine the order of magnitude of  $H_2S$  permeation and selectivity with respect to other gases. The focus was on confirming the facilitated transport mechanism involving  $H_2S$  reaction with the alkali carbonates and to determine the operating conditions under which measurable  $H_2S$  permeation could be obtained. A total of four membranes were investigated in this phase, each membrane being tested over a period of several days. The amount of salt infiltration in these membranes ranged from 72 to 82 percent by weight. Since this phase was more of a scoping study, only short-term experiments were conducted, i.e., a set of operating conditions was held constant only for a period of 1 to 4 hours. These membranes were kept molten during nontesting hours with a small flow of  $CO_2/N_2$  purge and sweep gases on both sides of the membranes. In general, membranes were found to be very dynamic in nature with small pressure fluctuations in the feed or sweep side causing immediate surges in concentrations of permeating species on the sweep side. A steady state was therefore found to be difficult to achieve during these short-term experiments. The permeation data collected during reasonably steady-state operations in these four runs are given in Table 3-2 along with the respective operating conditions.

Hydrogen and carbon monoxide concentrations were measured in the permeate stream along with  $H_2S$  concentrations to provide an indication of permeation across the membrane by porous viscous and diffusive flow mechanisms. Any  $H_2S$  transport in excess of that accounted by the porous viscous flow and diffusion mechanisms was considered to provide an indication of an enhanced facilitated transport of  $H_2S$ .

In all preliminary disc membrane experiments, dry feed gas composition corresponding to KRW coal gas was used which typically consisted of 18 percent  $CO$ , 12 percent  $H_2$ , 6 percent  $CO_2$ , 0.6 percent  $H_2S$  with balance  $N_2$ . The sweep gas consisted of 30 percent  $CO_2$  in  $N_2$ .

##### 3.1.1 Run No. 1

During loading of the first membrane to be tested in the membrane holder, a graphite tape wrapped around the ceramic membrane disc was found to provide a better seal than the "C" rings in the original membrane holder design (see Figure 2-2). This membrane was found to be very susceptible to small pressure fluctuations, e.g., those caused by draining of the condensate from the condensate separator catch-pot. Small changes in the transmembrane pressure drop were found to have a strong effect on the permeate concentrations indicating significant viscous flow contribution.

**Table 3-1. Percent Salt Infiltrations in the Membranes Used**

<b>Run No.</b>	<b>Membrane No.</b>	<b>Percent salt Infiltration by weight</b>
1	12496-13-1	80
2	12496-15-4	81
3	12496-13-3	82
4	12496-21-2	72
5	12496-21-5	72
6	12496-21-3	68
7	12496-23-5	68
8	12496-23-6	72
9	12496-23-8	67
10	12496-23-7	74
11	12496-24-5	65
12	12496-24-3	34
13	12496-24-1	69
14	12496-24-6	66
T-2	12496-26-T2	74
T-3	12496-26-T3	82
T-4	12496-26-T4	87.3

Table 3-2. Experimental Results of Preliminary Disc Membrane Experiments

Run No.	Date	Temp. (°C)	Pressure (psig)	Sweep gas flow rate dry scc/sec	Permeate conc. (ppm)				Permeability (Barrer x 10 <sup>-4</sup> )				Selectivity	
					H <sub>2</sub> S	COS	H <sub>2</sub>	CO	H <sub>2</sub> S	COS	H <sub>2</sub>	CO	H <sub>2</sub> S/H <sub>2</sub> (COS/H <sub>2</sub> )	H <sub>2</sub> S/CO (COS/CO)
1	10/28/92	570	50	21.7	30	0	NM	NM	82.9	—	—	—	—	—
	10/28/92	570	200	21.7	55	0	150	NM	45.8	—	6.4	—	7.2	—
	10/28/92	650	50	21.7	58	0	230	NM	60.2	—	32.4	—	4.9	—
	10/30/92	660	50	21.7	10	0	85	9	27.6	—	12.0	0.9	2.3	30.7
2	12/11/92	570	50	37.2	—	2.3	28	NM	—	11.1	6.9	—	1.6	—
	12/14/92	570	50	37.2	—	0.8	ND	NM	—	3.9	<0.7 <sup>a</sup>	—	>5.5	—
	12/14/92	605	50	37.2	—	1.1	ND	NM	—	5.3	<0.7 <sup>a</sup>	—	>7.6	—
	12/15/92	570	50	21.7	1.9	—	57	32	5.3	—	8.2	3.0	0.65	1.8
	12/15/92	570	100	21.7	3.6	—	94	28	5.7	—	7.7	1.5	0.74	3.8
4	1/27/93	560	53	33.1	0.45	—	ND	ND	1.9	—	<0.6 <sup>a</sup>	<1.4	>3.2	>1.4
	1/28/93	560	51	33.1	0.80	—	ND	ND	3.5	—	<0.7 <sup>a</sup>	<1.5	>5.0	>2.3
	1/28/93	560	200	39.1	1.0	—	ND	ND	1.6	—	<0.2 <sup>a</sup>	<0.5	>8.0	>3.2
	1/29/93	560	54	33.1	1.0	—	9	ND	4.0	—	1.8	<1.4	2.2	>2.9
	1/29/93	606	54	33.1	2.0	—	14	ND	8.2	—	3.0	<1.4	2.7	>5.9
5	2/4/93	560	52	33.1	0.51	—	ND	ND	2.0	—	<0.6 <sup>a</sup>	<1.4	>3.3	>1.4
	2/4/93	560	200	39.1	0.46	—	ND	ND	0.7	—	<0.2 <sup>a</sup>	<0.5	>3.5	>1.4

NM = Not measured.

ND = Not detected.

<sup>a</sup> Hydrogen and CO concentrations were assumed to be 3 and 10 ppm, respectively, equal to detection limits.

the transmembrane pressure drop were found to have a strong effect on the permeate concentrations indicating significant viscous flow contribution.

During the course of testing this membrane, it was discovered that in the absence of steam on the sweep side, carbonyl sulfide is liberated instead of H<sub>2</sub>S. This fact was easily explained by the reaction of CO<sub>2</sub> alone with the sulfide (S<sup>2-</sup>) ions in the melt instead of reaction given in Equation (1-1):



Gradual increase in H<sub>2</sub>S (or COS) concentrations was also often observed consistent with the reaction pathway and establishment of S<sup>2-</sup> ion concentration gradient across the membrane. Reasonably steady-state data were collected on only four occasions as shown in Table 3-2. In general, increasing system pressure was found to increase H<sub>2</sub>S concentration in the permeate stream; however, as data in Table 3-2 indicate, the permeability actually decreased with pressure consistent with the facilitated transport behavior. Increasing temperature was also found to increase the membrane permeability for H<sub>2</sub>S. The membrane performance, however, was found to degrade with time as seen from the second set of data obtained at the higher temperature.

The membrane permeability for H<sub>2</sub>S was quite high and ranged from 2.7x10<sup>5</sup> to 1.6x10<sup>6</sup> Barrers (1 Barrer = 10<sup>-10</sup> cm<sup>3</sup>-cm/cm<sup>2</sup>-s-cm of Hg). The measured H<sub>2</sub> permeabilities were also high and ranged from 6x10<sup>4</sup> to 1.2x10<sup>5</sup> Barrer units. The measured permeability for CO was about 9,000 Barrers. The expected permeability of hydrogen based on solution diffusion mechanism is of the order of only 200 Barrers. Thus, the high permeability for H<sub>2</sub> and CO indicates substantial leakage. The membrane still exhibited significantly higher selectivity for H<sub>2</sub>S when compared with H<sub>2</sub> and CO, indicating transport of H<sub>2</sub>S in excess of that accounted by leakage.

### 3.1.2 Run No. 2

The membrane used in this run was also found to be very dynamic and susceptible to small differential pressure changes. In the early part of this run, no gradual increase in H<sub>2</sub>S was observed on the permeate side with H<sub>2</sub>S containing coal gas on the feed side and 30 percent CO<sub>2</sub> sweep gas with steam on the permeate side. Similar to Run No. 1, steam was then turned off on the sweep side. After about 2 hours, at 570 °C and 50 psig conditions, COS was detected on the permeate side which began rising with time. Data collected after leveling off of permeate concentrations are shown in Table 3-2. Hydrogen concentrations in the permeate were also significant as seen from these data. On the next day, the effect of temperature was investigated on COS formation. Incidentally, on this day, hydrogen concentrations were below detection limit unlike the previous day. It appeared that, by keeping the membrane in purge gas, CO<sub>2</sub> atmosphere with negligible flows may seal any pores exposed during the flow testing conditions. Higher temperature operation increased the COS permeation. In general, the H<sub>2</sub>S and other permeabilities were much lower than those observed in Run No. 1 perhaps due to less leakage. H<sub>2</sub>S selectivities were also lower, except for the data collected on 12/14/92 when both H<sub>2</sub> and CO concentrations were found to be below detection limit.

On subsequent days, additional data were collected in the presence of steam on the sweep side with H<sub>2</sub>S being formed instead of COS. Significant CO and H<sub>2</sub> concentrations, however, were also observed as seen from data presented in Table 3-2. Eventually, H<sub>2</sub>S

concentrations in the permeate appeared to decrease with time, indicating degradation of membrane performance. One potential reason for membrane degradation is sulfate formation in the molten salt which reduces the amount of active species in the melt. Possible sources of oxygen include trace amounts in the sweep gas cylinders and dissolved oxygen in the water used to form steam. Oxygen-free sweep gases were used in the subsequent runs. Also the water reservoir was aerated with nitrogen in subsequent runs to remove dissolved oxygen from the deionized water.

### 3.1.3 Run No. 4

Run No. 3 was aborted because of the carbon formation during startup leading to plugging and no data were collected. The steady-state data obtained in Run No. 4 are shown in Table 3-2. KRW coal gas was used as feed gas and data were collected at two pressures and two temperatures. Operating conditions were kept constant for about 2 hours (by avoiding draining of condensate) before collecting steady-state data. The data collected for identical operating conditions on subsequent days appeared to be different, e.g., those on 1/27/93 and 1/28/93, indicating a need for a long-term continuous operation. During the overnight conditions of low purge and sweep CO<sub>2</sub> gas flows, the sulfide and carbonate ion concentrations within the melt apparently redistribute to achieve uniform concentrations. Thus, at the beginning of the next day, owing to the greater sulfide concentration on the permeate side of the membrane, the H<sub>2</sub>S concentration in the permeate is always found to be greater than that at the end of the previous day.

The data collected at 50 and 200 psig system pressures indicated reduction in H<sub>2</sub>S permeability at the higher pressure. This is generally consistent with the facilitated transport mechanism. Increasing membrane temperature was found to increase the H<sub>2</sub>S permeability significantly. The CO concentrations in the permeate were below detection limit throughout the duration of this run indicating good sealing of the membrane. Hydrogen concentrations were also below detection limit for the first few days. Run No. 4 was the first good run indicating H<sub>2</sub>S transport in the absence of any significant CO and H<sub>2</sub> transport, thus emphasizing the potential for significant H<sub>2</sub>S selectivity over H<sub>2</sub> in these membrane systems. Membrane degradation observed in Runs No. 1 and 2 appeared to be reduced in Run No. 4. The measured H<sub>2</sub>S permeabilities ranged from 16,000 to 82,000 Barrers well in excess of those expected by the solution diffusion mechanism.

### 3.1.4 Run No. 5

This run attempted to reproduce the results obtained in Run No. 4, using a new membrane. Steady-state data obtained at 50 and 200 psig system pressure at 560 °C are shown in Table 3-2. H<sub>2</sub>S permeation observed at 50 psig condition was similar to that observed in Run No. 4, whereas H<sub>2</sub>S permeation observed at 200 psig pressure was lower than in the previous run. Both the hydrogen and CO concentrations in the permeate was below the detection limit, thus indicating potentially high H<sub>2</sub>S selectivities for this membrane.

### 3.1.5 Summary and Discussion

The preliminary disc membrane experiments indicated significant H<sub>2</sub>S transport across the membrane and identified several interesting trends as summarized below:



- Permeability of the molten salt impregnated ceramic membranes was often greater for H<sub>2</sub>S than that for H<sub>2</sub> and CO, indicating enhancement of H<sub>2</sub>S transport over the porous viscous and diffusive flow mechanisms.
- Concentration of H<sub>2</sub>S in the permeate increases gradually before apparent leveling off. This fact is consistent with the reaction pathway for H<sub>2</sub>S transport and the time needed for diffusion of sulfide ions (S<sup>2-</sup>) within the liquid phase to establish a concentration gradient.
- In the absence of steam on the sweep side, COS is liberated instead of H<sub>2</sub>S. The concentration of COS was also seen to increase gradually with time. These observations are consistent with establishment of S<sup>2-</sup> ion concentration gradient in the liquid phase and subsequent reaction of S<sup>2-</sup> ions with CO<sub>2</sub> on the permeate side.
- Permeability of H<sub>2</sub>S was found to decrease with increasing feed pressure, consistent with facilitated transport of H<sub>2</sub>S. For conventional, solution diffusion mechanism, the permeability is expected to increase with the feed pressure.
- Permeability of H<sub>2</sub>S was found to increase with increasing temperature, presumably due to increased diffusivity of the S<sup>2-</sup> ions in the liquid phase.
- The susceptibility of the disc membranes to small changes in the transmembrane differential pressure, of the order of 1 to 2 psi, indicates either failure of the graphite seal at higher temperature or the presence of unfilled and/or relatively large pores in the ceramic membrane matrix which allow leakage of gases. (Approximate calculations indicate that 1 μm pores should be able to hold salt by capillary suction against 70 psi pressure differential.) The pressure fluctuations usually occurred with draining of the condensate. Thus, a continuous condensate draining system would be desirable to prevent system pressure upsets.
- The membrane often exhibited different steady states on subsequent days after keeping the membrane molten with low purge and sweep gas flow rates without steam. The H<sub>2</sub>S concentration in the permeate, in the presence of steam, was also usually higher at the beginning of a day as compared to that at the end of the previous day. During the overnight conditions of low purge and sweep CO<sub>2</sub> gas flows, the sulfide and carbonate ion concentrations within the melt apparently redistribute to achieve uniform concentrations. Thus, at the beginning of the next day, owing to the greater sulfide concentration on the permeate side of the membrane, the H<sub>2</sub>S concentration in the permeate is always greater than that at the end of the previous day. This observation indirectly corroborates the facilitated transport mechanism and identifies a need for a long-term continuous operation.
- In general, H<sub>2</sub>S concentrations in the permeate were low, less than a few parts per million. The H<sub>2</sub> and CO concentrations were often below detection limits of the detectors used. Thus, these preliminary experiments indicated a need for greater resolution in the GC analysis.

## 3.2 CONTINUOUS LONG-TERM DISC MEMBRANE TESTING

The purpose of the long-term disc membrane testing was to further substantiate facilitated transport mechanism for H<sub>2</sub>S permeation and to investigate membrane stability and performance over a long period of time. In these tests, the experimental system used during preliminary studies was modified to allow continuous operation as described in Section 2.1.2. In the preliminary experiments, permeation of H<sub>2</sub>S was compared with the permeation of H<sub>2</sub> and CO to determine the membrane selectivity with respect to H<sub>2</sub>S. However, both of these gas species may have alternative sources in addition to permeation through the membrane, e.g., H<sub>2</sub> may be formed by reaction of steam with the metallic parts of the membrane holder on the permeate side or even by decomposition of permeated H<sub>2</sub>S. Similarly, CO may be formed by reverse water gas shift reaction on the permeate side. In order to obtain quantitative determination of permeation due to porous viscous or diffusive flow mechanism, an inert gas, helium, was added to the coal gas in all of the long-term membrane experiments.

A total of nine disc membranes were tested in continuous long-term operation mode. The amount of salt infiltration in these membranes ranged from 65 to 74 weight percent except for a thicker membrane used in Run No. 12 which had only 34 percent salt infiltration. The modifications made to the condensate drain system virtually eliminated system pressure fluctuations, allowing operation at small controllable transmembrane differential pressures of 0 to 2 psi. More sensitive detectors were used in the GCs with a detection limit of 0.1 ppm for H<sub>2</sub>S and 2 ppm for both helium and hydrogen. With the system modifications, it was possible to maintain the same operating conditions over a period of days instead of a few hours as in the case of the preliminary experiments. The steady-state data obtained in the continuous long-term disc membrane tests are summarized in Table 3-3. The results obtained in each experiment are described below separately.

### 3.2.1 Run No. 6

During this first long-term run, steady-state membrane permeation data were obtained using two feed gas compositions: (1) similar to KRW coal gas with steam and (2) 2 percent H<sub>2</sub>S in N<sub>2</sub> without steam. The operating conditions were 50 psig pressure and 560 °C temperature and the corresponding data are presented in Table 3-3. Early on during this run, it became evident that a long time of several hours was needed to achieve steady-state membrane operation in contrast to the preliminary experiments. The primary difference in the long-term experiments and the preliminary experiments was the lack of pressure upsets in the long-term runs which usually caused sudden bursts of high H<sub>2</sub>S and other gas species concentrations in the preliminary experiments. Perhaps, these occasional high concentration leaks helped more rapid sulfidation of the salt layer and allowed a steady state in a shorter time in the preliminary experiments.

Both the steady-state data and the transient time dependent data could be used to determine the reaction equilibrium constant and the liquid phase diffusion coefficient as described in Section 4. After collecting the initial data, the molten salt in the membrane was accidentally solidified because of power failure which turned off the furnace. The salt was remelted and data were collected under conditions similar to the initial data as shown in Table 3-3. The membrane's ability to permeate H<sub>2</sub>S was found to be reduced as indicated by the higher temperature needed to obtain similar H<sub>2</sub>S permeation rate using coal gas as feed. The membrane degradation may be due to freezing and remelting process.

This page intentionally left blank.

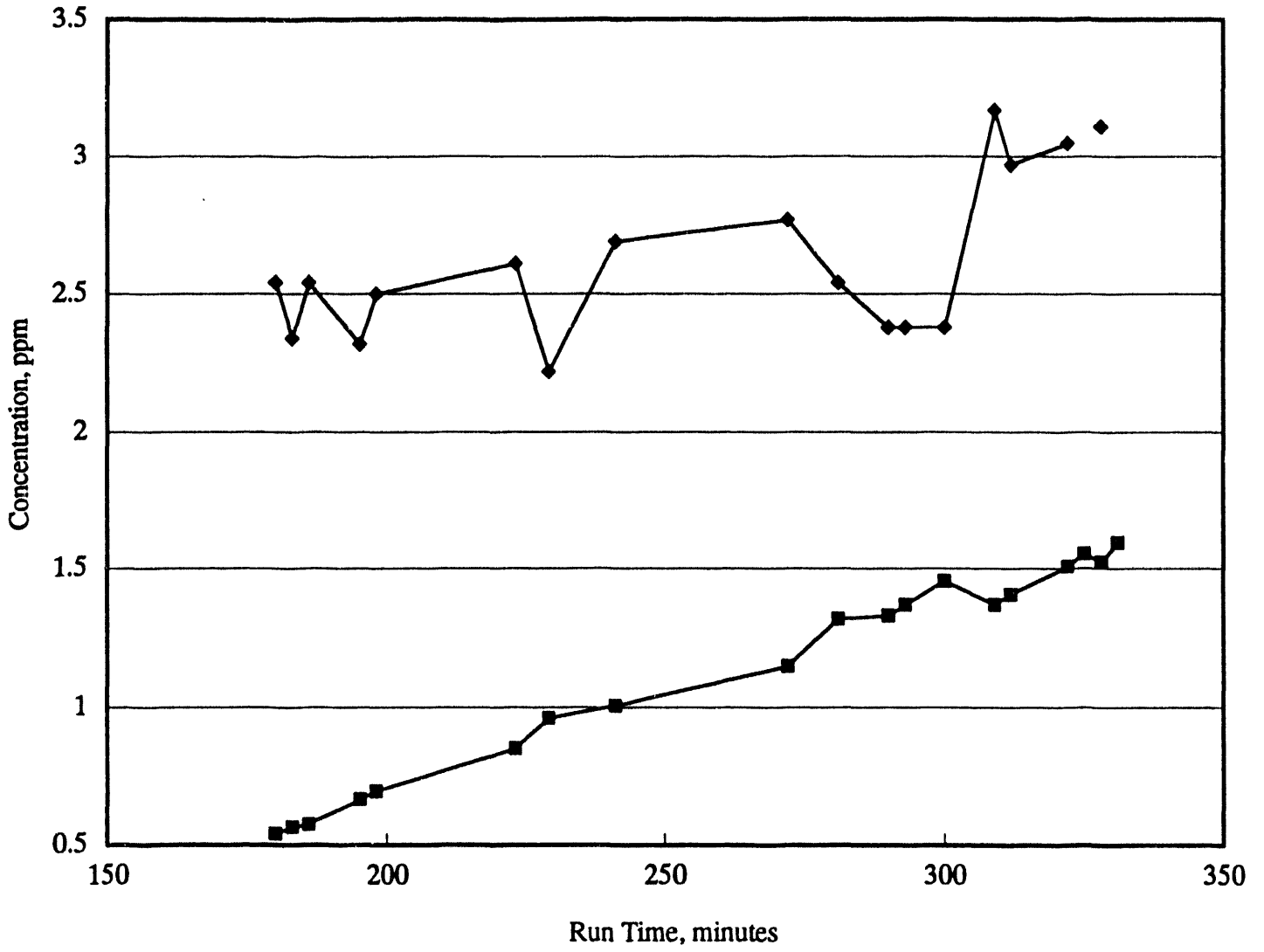


**Figure 3-1. Helium and H<sub>2</sub>S concentrations with time (Run #6, 5/3/93, 50 psig, 556 °C).**

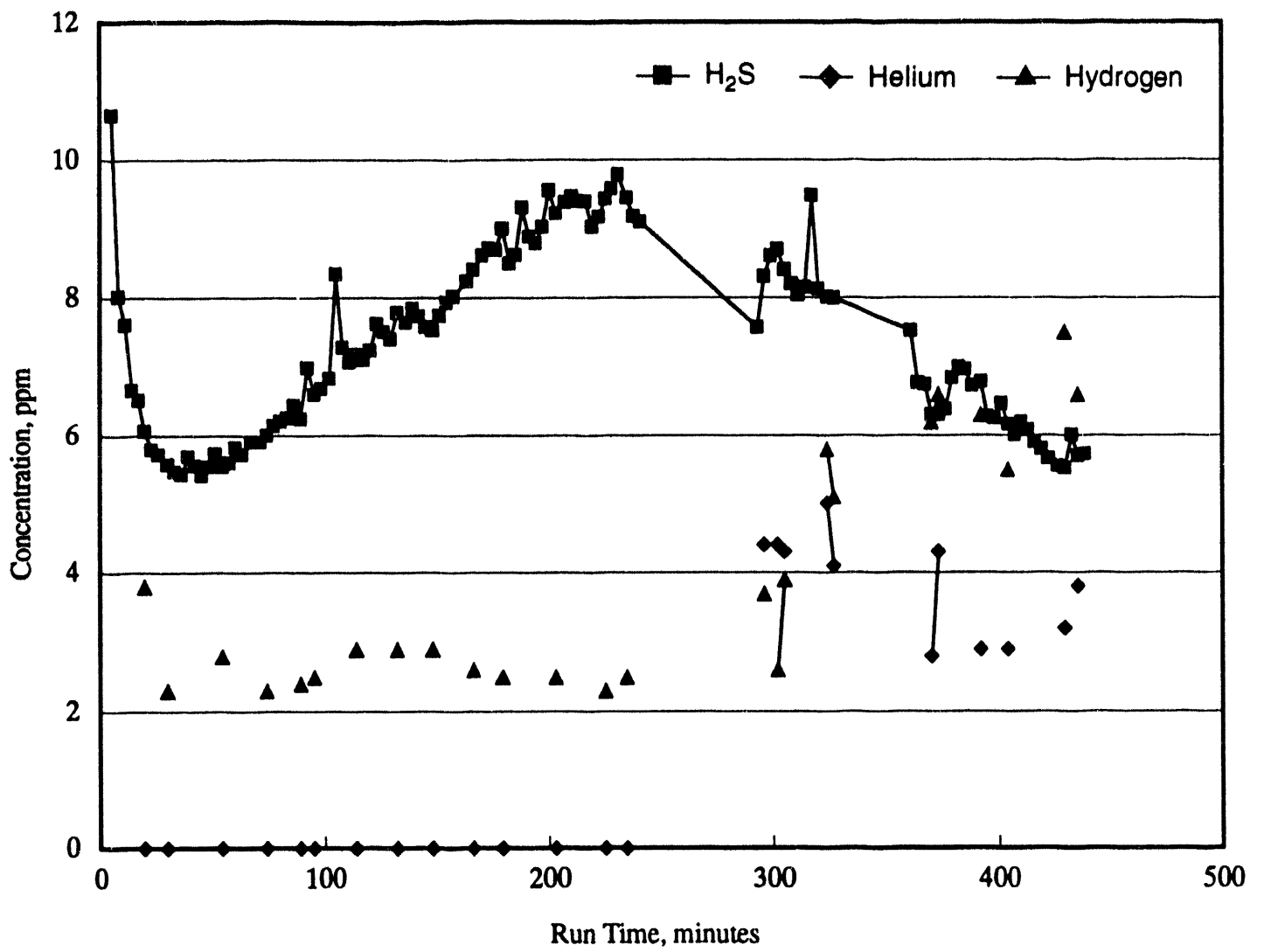


**Figure 3-2. Helium, hydrogen, and H<sub>2</sub>S concentrations with time (Run #6, 5/4/93, 50 psig, 556 °C).**

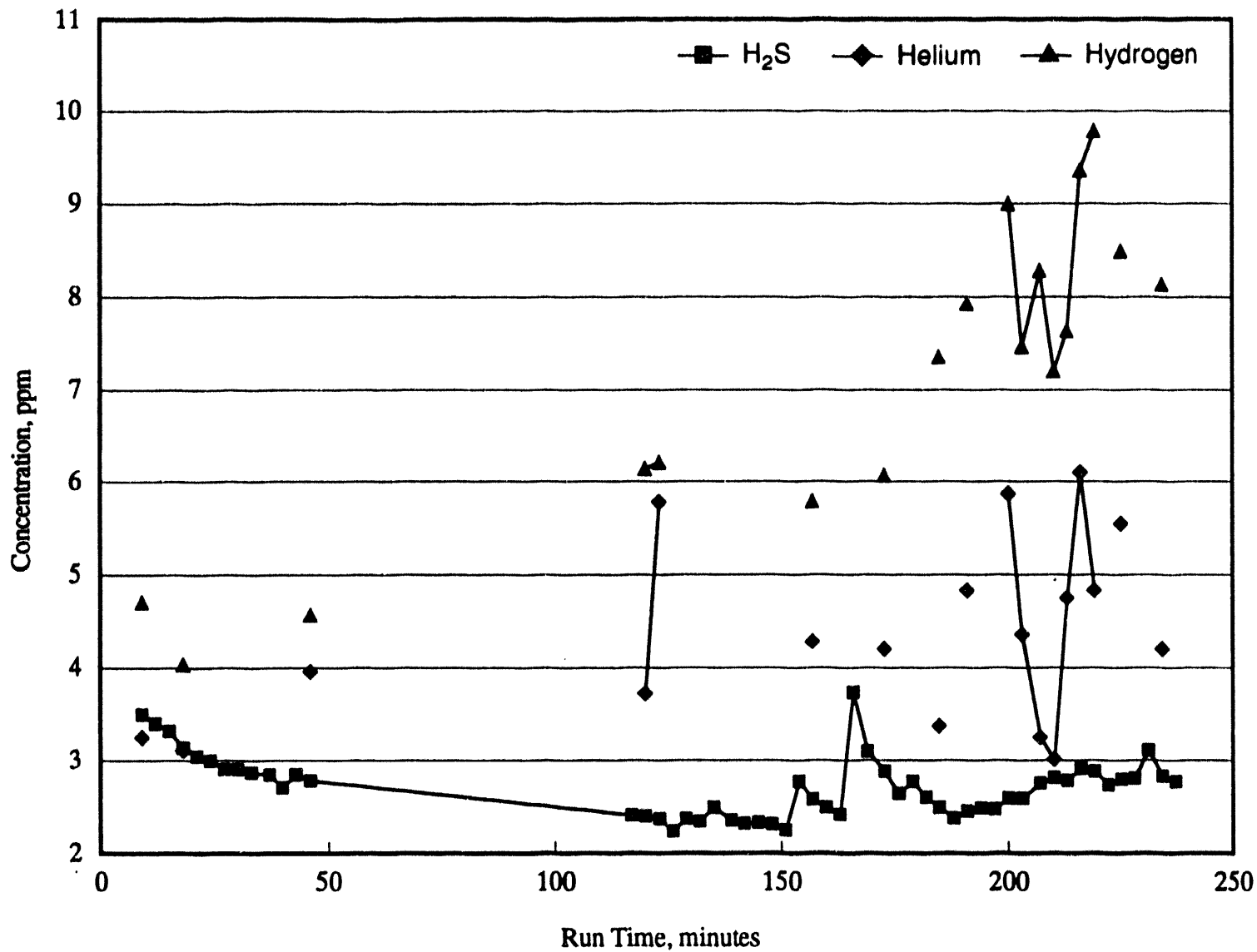


Figure 3-3. Helium, hydrogen, and H<sub>2</sub>S concentrations with time (Run #6, 5/5/93, 50 psig, 556 °C).

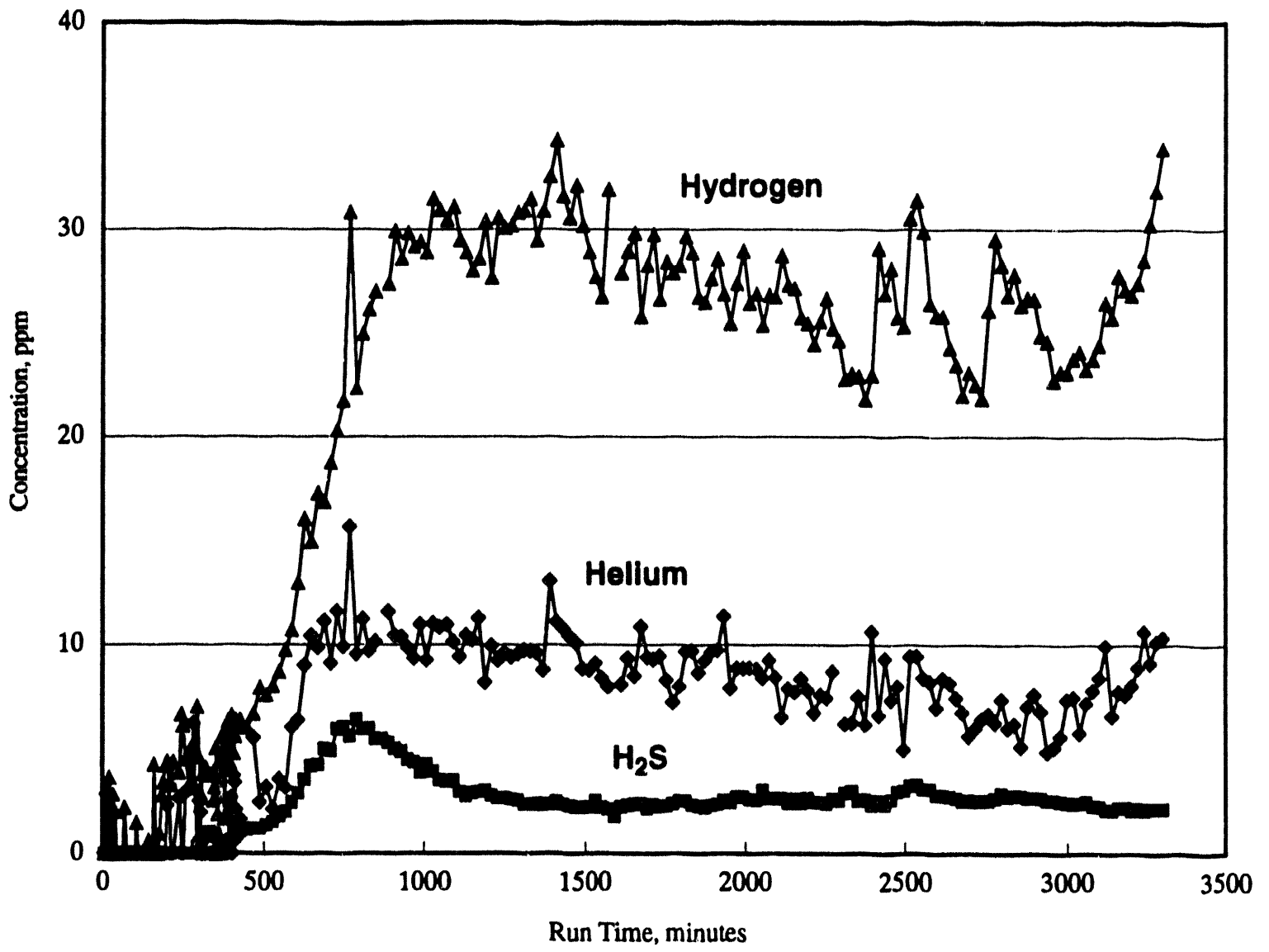


Figure 3-4. Helium, hydrogen, and H<sub>2</sub>S concentrations with time (Run #8, 6/4/93 – 6/6/93, 50 psig, 615 °C).

The membrane permeability for H<sub>2</sub>S ranged from 40,000 to 60,000 Barrers and the H<sub>2</sub>S selectivities with respect to hydrogen and helium were found to be 3.4 and 6.1, respectively. Both the helium and hydrogen concentrations were found to increase slowly with time in this run as seen in the concentration/time plots shown in Figures 3-1, 3-2, and 3-3 indicating a slow increase in the leakage rate with time. The transient H<sub>2</sub>S concentration data, e.g., that seen in Figure 3-1 may be used to estimate the liquid phase diffusion coefficient.

### 3.2.2 Run No. 7

This experiment was conducted with KRW coal gas with steam as feed gas and 30 percent CO<sub>2</sub> in N<sub>2</sub> as sweep gas. The system pressure and temperature were 50 psig and 560 °C, similar to the last run. This membrane did not indicate any H<sub>2</sub>S permeation over 6 hours, although helium and hydrogen concentrations in the permeate were significant. This run was therefore terminated. The reasons for the membrane inactivity were not clear. Incomplete salt penetration into the ceramic matrix leading to an inner zone of no salt is a possibility.

### 3.2.3 Run No. 8

This experiment was carried out with the feed gas composition similar to the KRW coal gas and was continued for almost 4 days from 6/4/93 to 6/7/93. The sweep gas composition and the steam flow rates were the same as in the previous runs. The membrane conditions were kept at 50 psig pressure and 615 °C for about 2½ days. As seen from the concentration/time plot shown in Figure 3-4, for the first 4 to 5 hours both helium and H<sub>2</sub>S concentrations in the permeate were negligible, and hydrogen concentrations were below 4 ppm. All three concentrations began rising in the permeate for the next 7 to 8 hours. The permeate H<sub>2</sub>S concentration went through a peak of about 6 ppm and then leveled off to about 2.7 ppm. The helium and hydrogen concentrations went through peaks of 10 and 30 ppm with mean concentrations of 8 and 26 ppm during the leveling off period for the H<sub>2</sub>S concentrations. The resulting selectivities of H<sub>2</sub>S permeation with respect to helium and hydrogen were about 3.4 and 1.04 respectively. The H<sub>2</sub>S selectivities at peak concentrations were about 5.9 and 2.4, respectively.

The reasons for much higher hydrogen concentrations than helium concentrations were not clear. Decomposition of permeated H<sub>2</sub>S may partially account for the higher hydrogen concentrations. It is interesting that the peaking of hydrogen and helium concentrations occurred soon after the peaking of H<sub>2</sub>S concentration.

At the end of the 2½ day run, it was apparent that there was significantly more pressure drop on the sweep side of the membrane holder. At this time the temperature was reduced to 575 °C; however, the pressure drop continued to increase with time. An attempt was made to obtain permeation data at a higher system pressure of 200 psig. However, a leak was developed in the membrane during pressurization on both sides of the membrane. By the time the membrane was stabilized the sweep side pressure drop had become excessive and the run was aborted. Upon disassembly of the membrane, the sweep side pressure drop was attributed to oozing of the molten salt on the sweep side (which was also the bottom side) and blocking the gas flow in the small gas flow clearance space. The oozing of the salt from the membrane pores due to gravity indicates presence of some pores much greater than 1 μm. In order to prevent such blockage in future experiments, the gas flow clearance on the sweep (bottom) side of the membrane holder was increased by increasing the depth of the recessed space in the membrane holder.



### 3.2.4 Run No. 9

This run was carried out on 6/23/93 to 2/4/93, with experimental parameters of 600 °C temperature and 50 psig pressure. The experimental conditions were maintained constant for about 5 hours until the end of the day, and the testing was continued overnight. H<sub>2</sub>S and helium concentrations began to appear in the sweep gas after about 3 hours. For the next 6 to 7 hours H<sub>2</sub>S and H<sub>2</sub> concentrations increased continuously to about 9 and 20 ppm, respectively, whereas helium concentrations stabilized to about 3 to 4 ppm. At this point, apparently a leak was developed in the membrane resulting in very high concentrations of permeating species in the sweep gas. Although the run continued, the measured concentrations were erratic. The next morning, the system pressure was found to have increased to about 140 psig (from 50 psig). A filter before the BPR was found to be clogged causing the pressure increase. This run was therefore aborted, although the membrane was kept molten with purge CO<sub>2</sub>/N<sub>2</sub> gas mixtures flowing on both sides. The clogged filter element was removed. All the filter elements made for 1/8 in. tube fittings were replaced with larger filter elements made for 1/4 in. tube fittings.

The concentrations prior to the system upset are shown in Figure 3-5. The final concentrations in this plot were used to estimate the membrane permeabilities and selectivities. As seen from the Table 3-3, the H<sub>2</sub>S permeability at this point was about  $2 \times 10^5$  Barrers. The membrane selectivities for H<sub>2</sub>S with respect to helium and hydrogen were about 18 and 11.

The membrane used in the previous run was reused on 6/28/93 with identical experimental conditions. However, within the first 3 hours it became apparent that on the test side of the membrane holder there was an excessive pressure drop and it was impossible to balance the pressures on both sides of the membrane. The run was therefore aborted. Upon disassembly of the membrane, the feed side pressure drop was attributed to carbon deposits on the membrane near the inlet feed gas opening blocking the gas flow. Carbon may form if the steam concentration is not adequate to prevent reverse gasification reactions. In order to determine the effect of feed side steam concentration on carbon formation, a dummy run was made on June 30 using a stainless-steel disc instead of the membrane and a feed side steam concentration of 25 percent by volume. All other conditions were the same as in this run. The membrane differential pressure gauge was monitored for any evidence of increased pressure drop on the feed side. The differential pressure remained constant over a 6-hour period indicating a stable system operation. No helium or hydrogen was detected in the sweep outlet gas.

### 3.2.5 Run No. 10

This run was carried out on 7/6/93 to 7/9/93 with experimental parameters of 600 to 640 °C temperature and 50 psig pressure. Thirty percent CO<sub>2</sub> in N<sub>2</sub> was used as sweep gas. The steam content in sweep gas was about 16.7 percent. Due to high CO and H<sub>2</sub> concentrations in the coal gas used, steam concentration in the membrane feed gas was maintained at about 25 percent to minimize carbon formation. The temperature was initially maintained at 600 °C. This membrane did not indicate any significant H<sub>2</sub>S permeation for first 24 hours except for a brief period of H<sub>2</sub>S concentrations in sweep gas of 0.2 ppm. The temperature was, therefore, increased to about 640 °C to increase membrane activity. The helium concentration in the sweep gas was negligible for first 16 hours indicating good sealing of the membrane. The helium concentration then increased to about 5 ppm in the next 8 hours. After raising the membrane temperature, H<sub>2</sub>S concentration reached a steady-state level of 0.54 ppm in sweep gas in about 5 hours. The H<sub>2</sub>S concentrations remained at this level for about 5 hours and then declined to

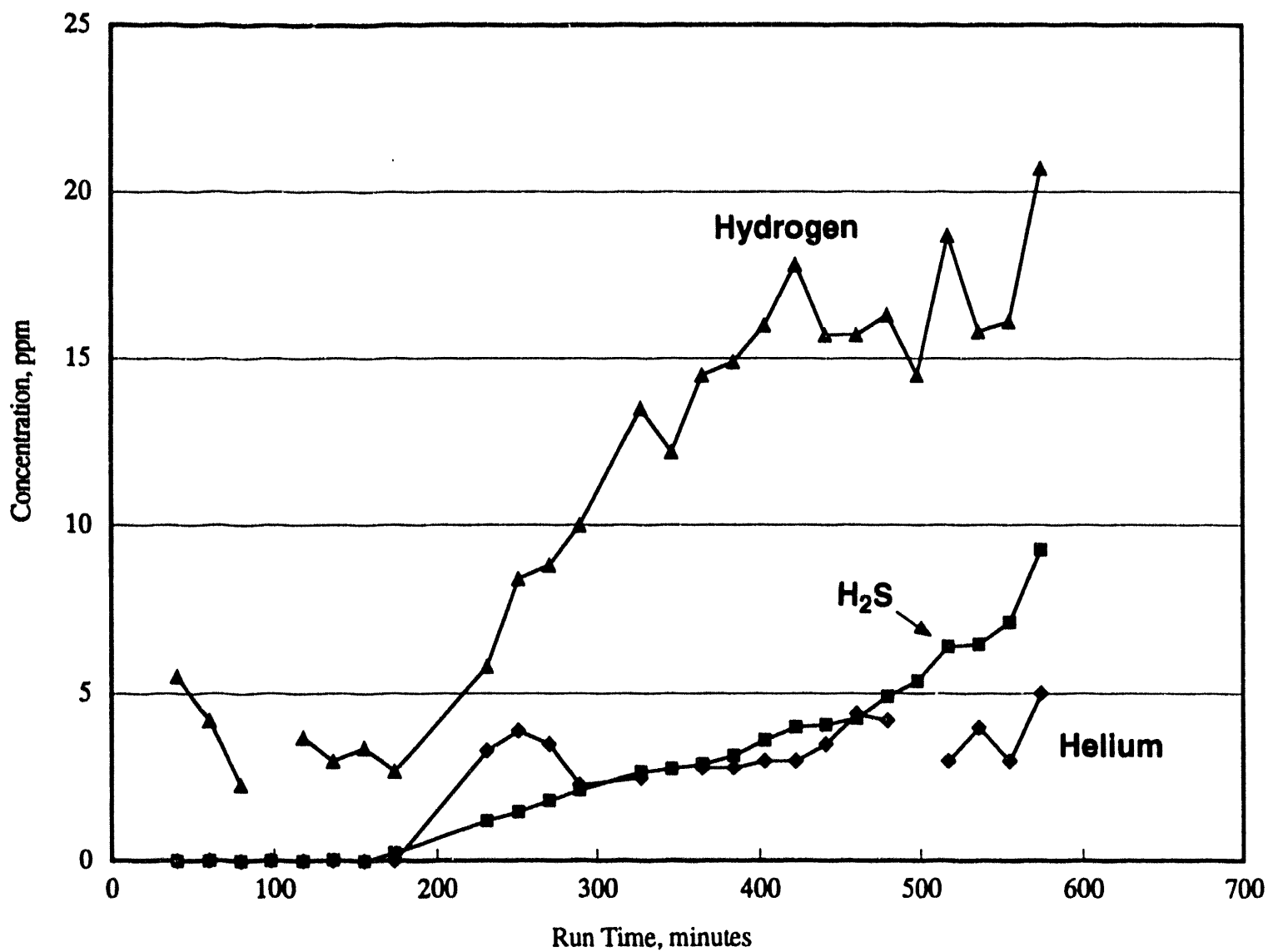


**Figure 3-5. Helium, hydrogen, and H<sub>2</sub>S concentrations with time (Run #9, 6/23/93, 50 psig, 600 °C).**

about 0.3 ppm in next 6 to 7 hours. At this point the steam concentration on the feed side was decreased to 15 percent which increased the H<sub>2</sub>S concentration to another steady-state level of 0.66 ppm where it remained for about 4 hours. Helium concentrations in the sweep gas, however, also increased at the same time to about 12 ppm. The membrane temperature was then decreased to 600 °C to determine the effect of temperature on membrane performance. The sweep gas H<sub>2</sub>S concentration decreased to about 0.4 ppm and remained at this level for next 3 hours and then decreased to less than 0.1 ppm in next 3 hours. During the same time helium concentrations increased to about 20 ppm.

The observed H<sub>2</sub>S selectivity of the membrane with respect to helium was only 1.3 during the 5 hour steady-state period at 640 °C with H<sub>2</sub>S permeability of 13,000 Barrers. The hydrogen concentrations in the sweep gas were consistently higher than helium with a hydrogen selectivity with respect to helium of about 1.9 during the latter half of the experimental run.

### **3.2.6 Run No. 11**

This run was conducted on 8/4/93 to 8/7/93. A mixed coal gas composition consisting of 24.6 percent H<sub>2</sub>, 29.3 percent CO, 10.4 percent CO<sub>2</sub>, 6.6 percent He, 0.9 percent H<sub>2</sub>S, and balance N<sub>2</sub> was used as feed gas. The membrane was maintained at 607 °C and the system pressure was varied from 50 to 150 psig. Thirty percent CO<sub>2</sub> in N<sub>2</sub> was used as sweep gas. The steam content in sweep gas was about 26 percent. Due to high CO and H<sub>2</sub> concentrations in the coal gas used, steam concentration in the membrane feed gas was maintained at about 25 percent to minimize carbon formation. At the initially 50 psig system pressure, a steady state was observed after about 19 hours with steady concentrations of H<sub>2</sub>S, helium, and H<sub>2</sub> of 1.4 ppm, 19 ppm, and 135 ppm, respectively. The selectivity of H<sub>2</sub>S with respect to helium was about 0.6 with H<sub>2</sub>S permeability of 23,000 Barrers. After increasing the system pressure to 100 psig, the H<sub>2</sub>S concentrations first reached an apparent steady-state level of 2.1 ppm which held for several hours, resulting in H<sub>2</sub>S permeability of 19,000 Barrers. The H<sub>2</sub>S concentration then declined continuously. The helium and hydrogen concentrations were stable at approximately 20 ppm and 150 ppm, respectively. Upon increasing the system pressure to 150 psig, both the helium and hydrogen concentrations in the permeate increased, whereas the H<sub>2</sub>S concentration declined continuously. The membrane was believed to be slowly deactivating, and the run was terminated after 75 hours of total operation.

### **3.2.7 Run No. 12**

This run was conducted with one of the thicker membranes on 8/16/93 to 8/19/93. KRW coal gas composition consisting of 12.3 percent H<sub>2</sub>, 6.4 percent He, 17.6 percent CO, 6.2 percent CO<sub>2</sub>, 0.67 percent H<sub>2</sub>S, and balance N<sub>2</sub> was used as feed gas. 30 percent CO<sub>2</sub> in N<sub>2</sub> was used as sweep gas. The steam content in sweep gas was about 26 percent. The steam concentration in the membrane feed gas was maintained at about 25 percent to minimize carbon formation. The temperature was maintained at 605 °C and the system pressure was maintained at 50 psig. No H<sub>2</sub>S was detected in the permeate during a 60-hour run although significant amounts of helium and hydrogen were found in the permeate. The run was terminated after 60 hours. The membrane used in this run cracked during disassembly. The exposed cross section of this membrane indicated incomplete penetration of salt into the membrane.

### 3.2.8 Run No. 13

This experimental run was conducted with the thin membrane with identical conditions as in Run No. 12 on 8/24/93 to 8/25/93. In this run also, no H<sub>2</sub>S was detected in the permeate although a significant concentration of helium and hydrogen was present in the permeate. This run was terminated after 24 hours.

### 3.2.9 Run No. 14

This run was conducted on 8/30/93 to 9/4/93. Due to the lack of H<sub>2</sub>S permeation in the last two runs using coal gas, this run was begun with 2.9 percent H<sub>2</sub>S in nitrogen as feed gas. The membrane temperature was maintained at 560 °C and no steam was added to the feed gas. Thirty percent CO<sub>2</sub> in N<sub>2</sub> was used as sweep gas with about 15 percent steam. The system pressure was initially maintained at 50 psig. The first trace of H<sub>2</sub>S appeared in the permeate after about 8 hours. The H<sub>2</sub>S concentration then steadily increased to reach a steady-state level of about 17 ppm. The system pressure was then raised to 100 psig. The same level of the steady-state concentration was again reached. The system pressure was then increased to 200 psig. The H<sub>2</sub>S concentration again appeared to be steady at about 17 ppm, consistent with facilitated transport mechanism. These data are shown in Table 3-3.

The feed gas was then changed to the typical KRW coal gas composition. The steam content on the test side was about 25 percent and that on the sweep side was about 26 percent. The membrane temperature was again maintained at 560 °C and the system pressure was decreased to 50 psig. H<sub>2</sub>S concentration in the permeate decreased to a new steady-state level of 4.3 ppm with helium and H<sub>2</sub> concentrations of 5.5 ppm and 35 ppm, respectively. The H<sub>2</sub>S selectivity with respect to helium was about 7 and that with respect to hydrogen was about 2.5. The H<sub>2</sub>S permeability was about 92,000 Barrers. The system pressure was then raised to 100 psig. The new apparent steady-state concentrations of H<sub>2</sub>S, helium, and H<sub>2</sub> were about 3 ppm, 7.5 ppm, and 47 ppm, respectively. The selectivity of H<sub>2</sub>S with respect to helium decreased to about 4 and that with respect to hydrogen to only 1.1. The concentration/time for this run are shown in Figures 3-6 and 3-7.

Finally, the system pressure was then raised to 200 psig. After several hours, the transmembrane pressure drop increased substantially indicating an obstruction to gas flow on the sweep side of the membrane holder. No steady-state data could therefore be obtained at 200 psig condition. The run was terminated after 110 hours of operation. Upon disassembly of the membrane holder, the gas flow blockage was attributed to oozing of the molten salt from the membrane around the gas flow opening.

### 3.2.10 Summary and Discussion

The long-term testing of the disc membranes in Runs No. 6 through 14 produced mixed results. Enhanced H<sub>2</sub>S transport was observed in Runs No. 6, 8, 9, and 14, as evidenced by H<sub>2</sub>S selectivities of greater than unity with respect to helium and hydrogen. Membranes used in Runs No. 7, 12, and 13 did not indicate any H<sub>2</sub>S transport at all, whereas those used in Runs No. 10 and 11 produced poor selectivity. As seen in Table 3-1, all of these membranes had about the same amount of salt infiltration in the range of 65 to 74 percent by weight except for the thicker membrane used in Run 12 with only 34 percent by weight salt infiltration. Inspection of the cross section of the membrane used in Run No. 12 indicated an inner continuous zone of no salt

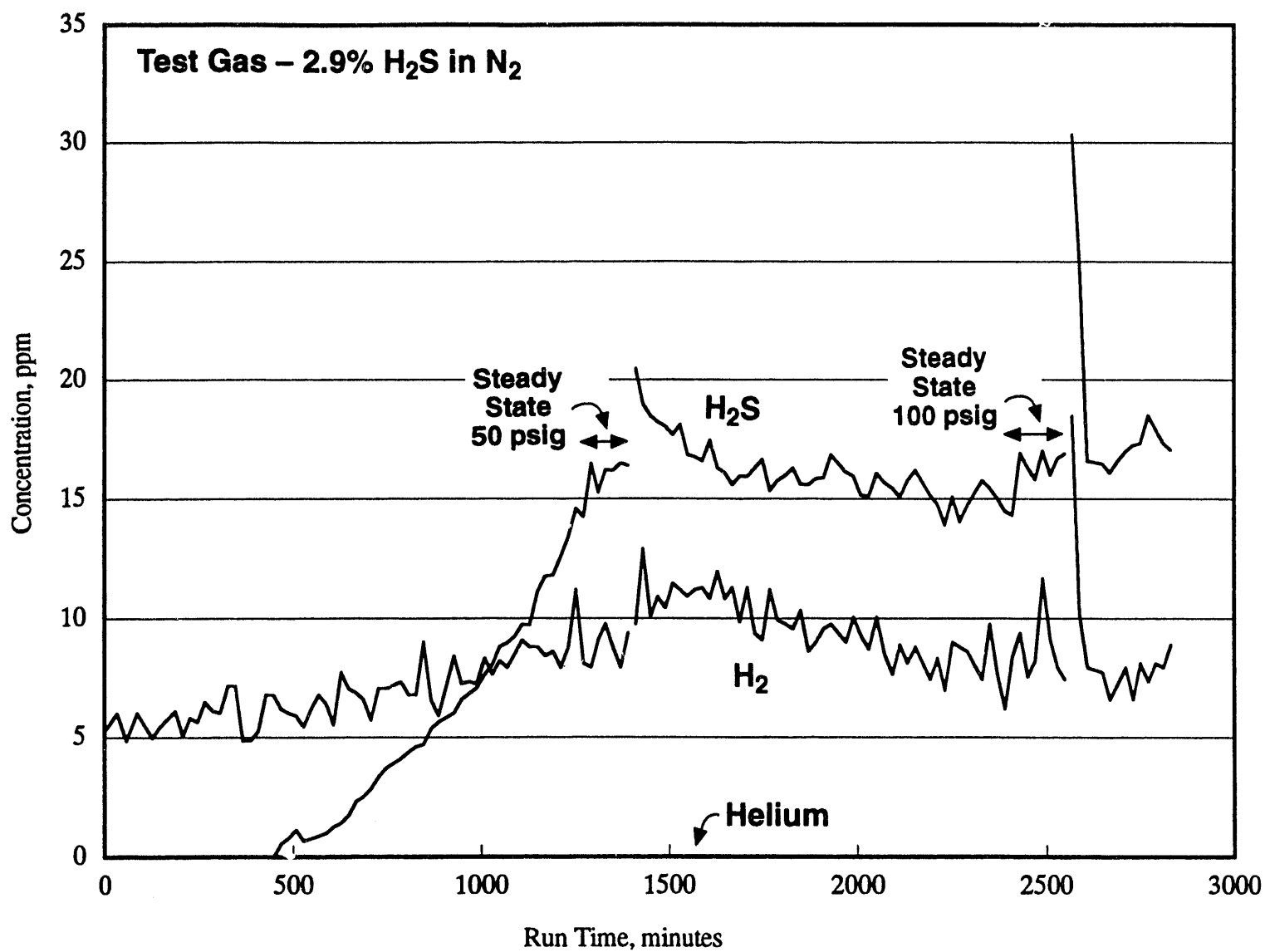


**Figure 3-6. Helium, hydrogen, and H<sub>2</sub>S concentrations with time (Run #14, 8/30/93 – 9/1/93, 50, 100, 200 psig, 560 °C).**

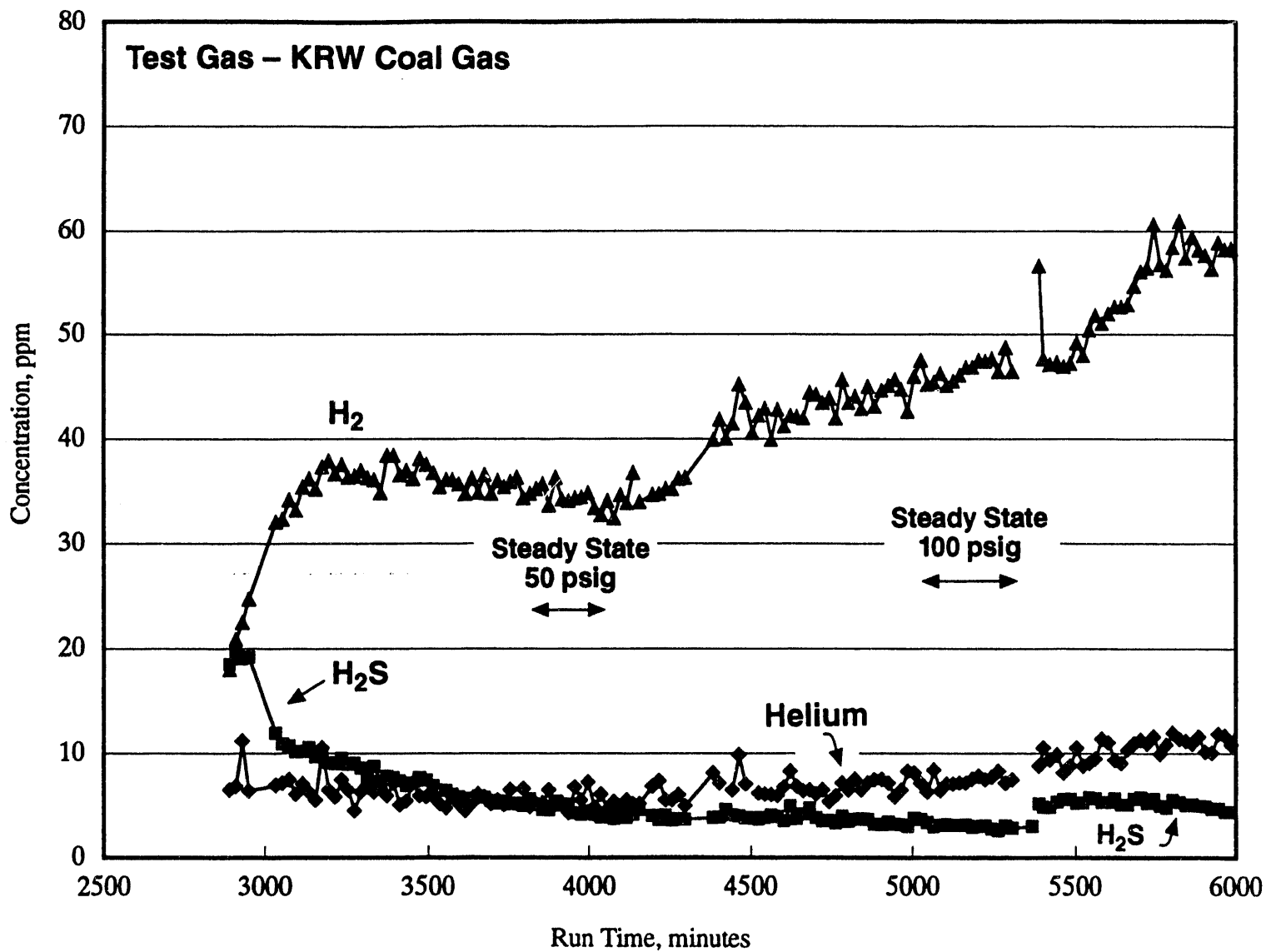


**Figure 3-7. Helium, hydrogen, and H<sub>2</sub>S concentrations with time (Run #14, 9/1/93 – 9/4/93, 50, 100, 200 psig, 560 °C).**

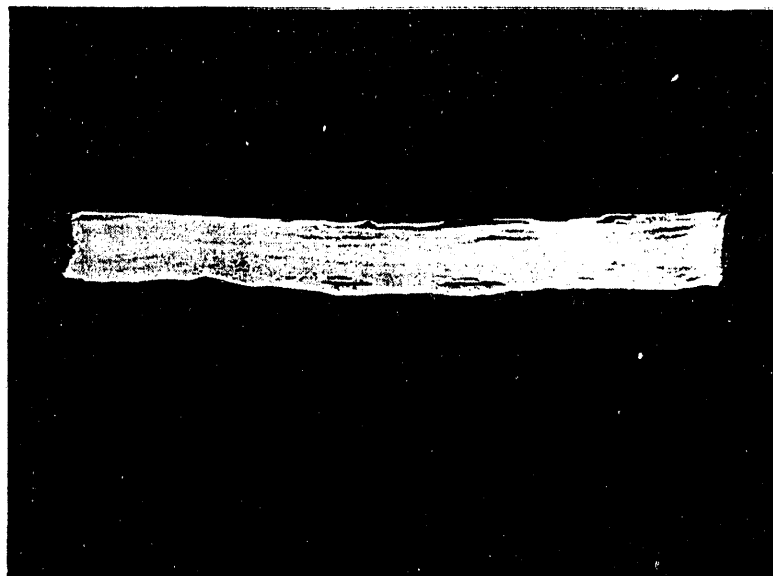
infiltration. Figures 3-8(a) and 3-8(b) clearly show an inner zone of no salt infiltration in a cross section of an unused thicker membrane which had cracked during the loading process. A similar zone of incomplete salt infiltration is also evident, as seen in Figures 3-9(a) and 3-9(b), in the cross section of a membrane used in Run No. 10 which had exhibited poor H<sub>2</sub>S selectivity. The cross sections of membranes used in Runs No. 6 and 8, which had shown enhanced H<sub>2</sub>S transport, also indicate non-uniform salt infiltration as seen by pockets of no salt infiltrations in Figures 3-10(a), 3-10(b), 3-11(a), and 3-11(b).

For enhanced facilitated H<sub>2</sub>S transport it is essential to have a continuous liquid phase exposed to feed and sweep gases on the two sides of a membrane. Any zones of discontinuity will obviously hinder the facilitated transport of H<sub>2</sub>S by the reaction pathway. The extreme case of a continuous inner zone of no salt infiltration will completely prevent the facilitated transport of H<sub>2</sub>S. In such an extreme case, the molten carbonate salt on the sweep side of the membrane will simply act as a scavenger for any H<sub>2</sub>S leaking through the porous flow, thus explaining the presence of significant helium and hydrogen permeate concentrations without any measurable permeate H<sub>2</sub>S concentrations in Run No. 12.

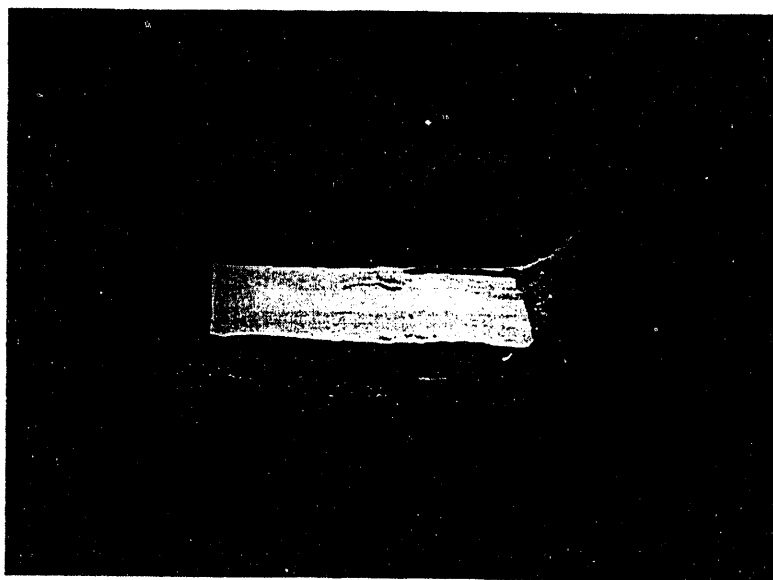
The nonuniformities in salt infiltration will also reduce the effective membrane cross-sectional area for H<sub>2</sub>S transport, thus affecting the calculated membrane permeabilities. The membrane H<sub>2</sub>S permeabilities observed in Runs No. 6, 8, 9, 10, 11, and 14 reflect a broad range in the calculated permeabilities that were based on a fixed membrane cross-sectional area. The calculated permeabilities for H<sub>2</sub>S ranged from 13,000 to 200,000 Barrers. On the other hand, the observed helium permeabilities, which essentially provide an indication of leakage flow, ranged from 10,000 to 40,000 Barrers with most of the values about 10,000 Barrers. The H<sub>2</sub>S to He selectivities for these runs were greater than unity except for Run No. 11 and ranged from 0.6 to 18. Hydrogen permeabilities were greater than those for helium, generally by a factor of two or more, and ranged from 18,000 to 79,000 Barrers. The corresponding H<sub>2</sub>S selectivities with respect to hydrogen were lower and ranged from 0.3 to 11.

The overall results obtained in the long-term membrane testing are summarized below:

- Enhanced transport of H<sub>2</sub>S was observed in several of the membranes tested with H<sub>2</sub>S permeabilities in the range of 13,000 to 200,000 Barrers and H<sub>2</sub>S to helium selectivities ranging from 0.6 to 18.
- Hydrogen permeabilities were greater than those for helium, generally by a factor of two, and ranged from 18,000 to 79,000 Barrers. The corresponding H<sub>2</sub>S selectivities with respect to hydrogen were lower and ranged from 0.3 to 11.
- Unlike the preliminary disc membrane experiments, the relatively stable operating conditions in the long-term experiments required much longer time, of the order of several hours, to achieve steady-state permeate concentrations. This time requirement indicates a very slow liquid phase diffusion process which also limits the observed H<sub>2</sub>S flux rates.
- The gradual increase in the permeate H<sub>2</sub>S concentrations is consistent with the reaction pathway for H<sub>2</sub>S transport and the time needed for diffusion of sulfide ions (S<sup>2-</sup>) within the liquid phase to establish a concentration gradient.



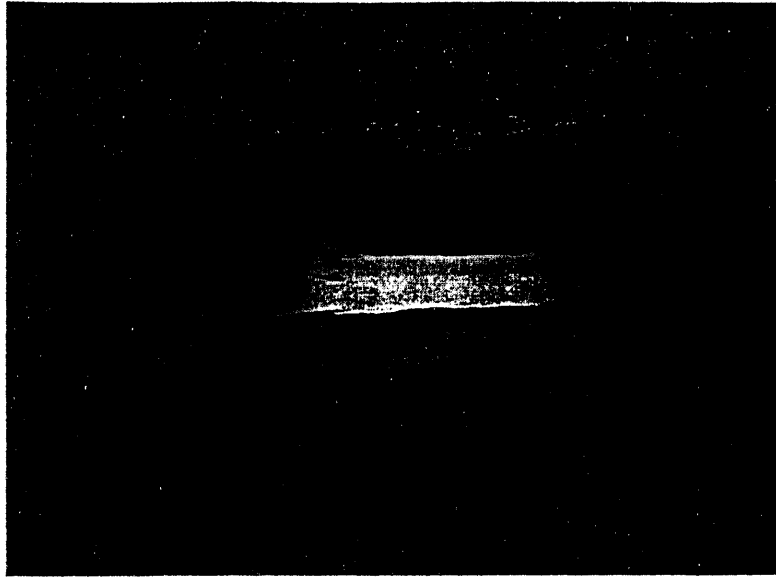
(a)



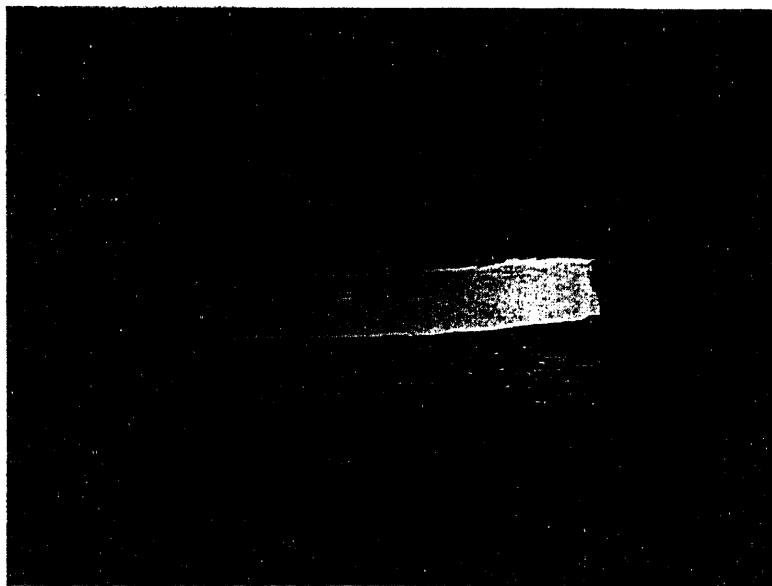
(b)

**Figure 3-8. Cross section of an unused thicker membrane.**



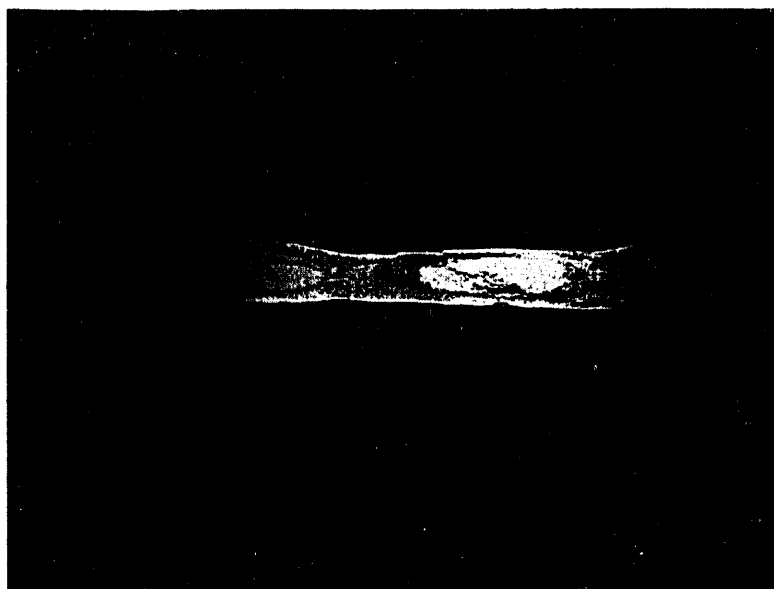


(a)

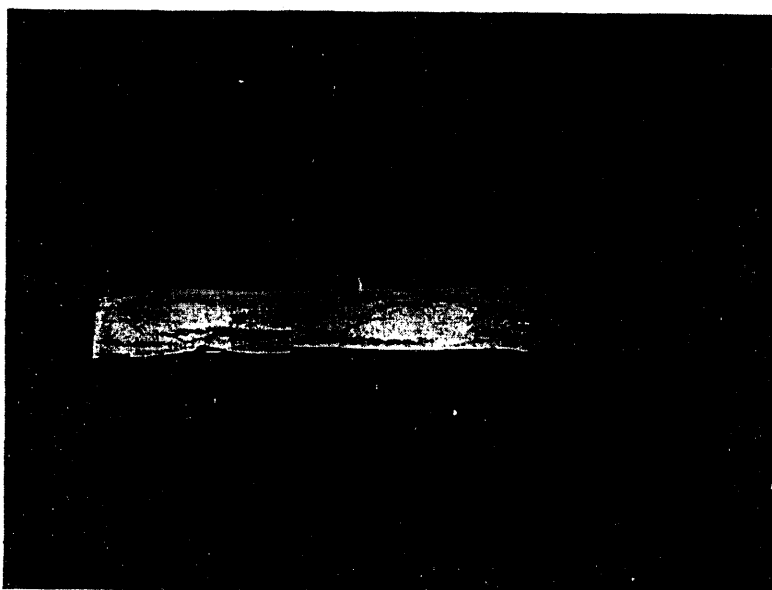


(b)

**Figure 3-9. Cross section of a membrane used in Run No. 10.**

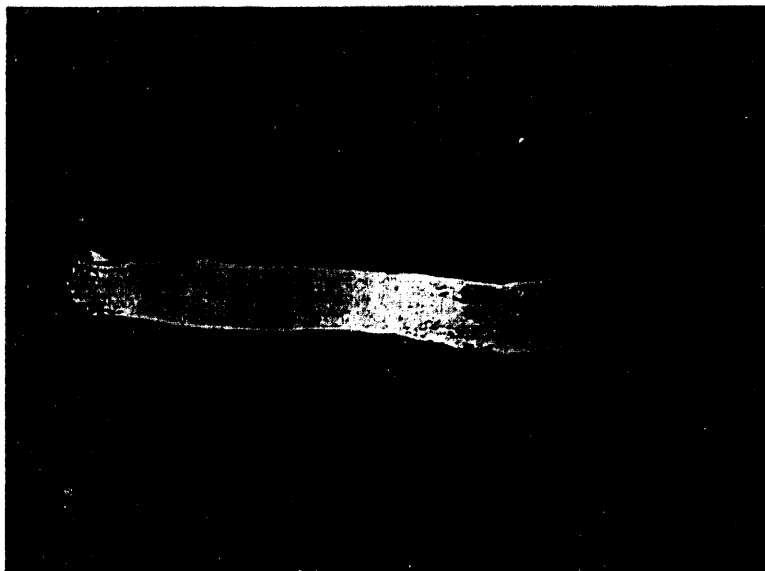


(a)

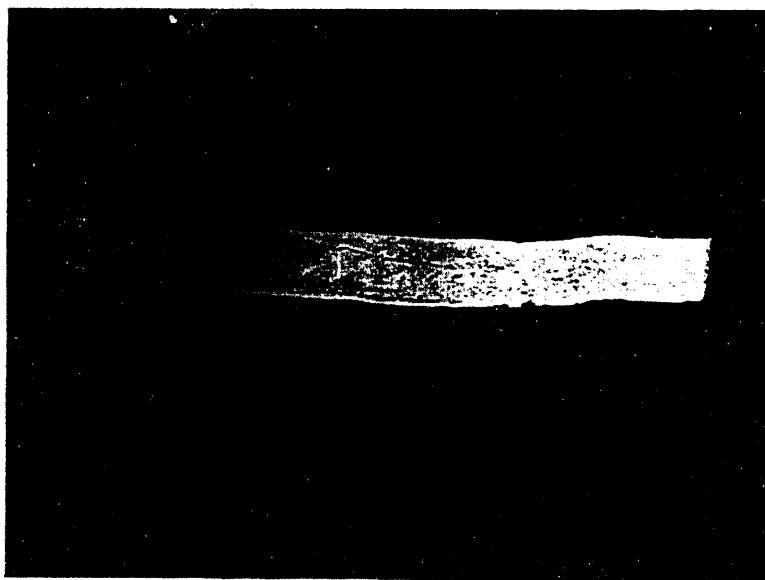


(b)

Figure 3-10. Cross section of a membrane used in Run No. 6.



(a)



(b)

**Figure 3-11. Cross section of a membrane used in Run No. 8.**

- Increasing system pressure was consistently shown to reduce H<sub>2</sub>S permeability, corroborating a facilitated transport process.
- The inconsistencies in the performance of different membranes may be explained by incomplete or nonuniform salt infiltration in the ceramic porous matrix.
- Helium and hydrogen concentrations generally increased over a long period of operation at a given temperature. This fact coupled with the observations of salt oozing from the membrane by gravity indicates the presence of large pores in the ceramic matrix unable to hold the salt in pores by capillary suction.

### **3.3 CONTINUOUS LONG-TERM TUBULAR MEMBRANE TESTING**

The observed permeate H<sub>2</sub>S concentrations in the long-term disc membrane experiments were low, ranging from 0.5 ppm to 9 ppm for coal gas conditions. Therefore, leakage due to the porous flow (viscous and diffusion) can have a substantial effect on the observed membrane performance. One source of leak is the graphite seals. The effect of leakage on the observed membrane performance can be minimized by increasing the membrane surface area. A tubular membrane offers a large membrane surface area while limiting the contribution by leakage at the seals. Membrane experiments with a tubular geometry that can increase the H<sub>2</sub>S flux rates while minimizing leakage are thus desirable to assess the performance of the molten salt membranes.

The tubular membranes used in these studies were about 15-mm dia and 3.5-mm thick and ranged from 8 to 10 in. in length. During salt infiltration, the inside of the tube was blocked from the salt by graphite rods, i.e., the molten salt was infiltrated only from outside of these tubes. Custom-made 15-mm graphite ferrules allowed sealing the tube ends in 15 mm to 1/2 in. reducing unions. A total of three membrane tubes were tested for membrane performance in continuous long-term tests. The membrane permeability and selectivity data collected in these tests are shown in Table 3-4.

#### **3.3.1 Run No. T-2**

Shakedown tests (Run No. T-1) were first conducted using a blank, unimpregnated membrane tube to test the tubular membrane reactor assembly. Run No. T-2 was the first test conducted with a salt-impregnated membrane tube and was carried out over 5 days on 11/17/93 to 11/22/93. A small leak flow through the tube was observed at 20 psi pressure differential during the cold pressure test. The test run began with 30 percent CO<sub>2</sub> on both sides of the membrane at 50 psig pressure and 560 °C temperature. The initial hydrogen leak rate through the tube was determined by using a KRW clean coal gas (without H<sub>2</sub>S) as a feed gas and was found to produce about 35-ppm concentration in the sweep outlet gas. The feed gas was then switched to the KRW coal gas with H<sub>2</sub>S. During the first 24 hours, the hydrogen, helium, and H<sub>2</sub>S concentrations increased substantially. The increase in sweep outlet concentrations was thought to be due to the downward gravitational flow of molten salt within the tube leading to opening of pores in the upper section of the tube. The temperature was then decreased to 500 °C. Relatively stable sweep outlet gas concentrations were observed during the next 16 hours. The H<sub>2</sub>S selectivity with respect to helium was about 1.6 during this period. The selectivity with respect to hydrogen was about 1 during the same period. The system pressure was then increased to 100 psig. For the next 9 hours the sweep outlet helium and hydrogen concentrations began to increase, whereas H<sub>2</sub>S concentration decreased slightly. At this point, during the over-

**Table 3-4. Experimental Results of Continuous Long-term Tubular Membrane Experiments**

Run No.	Date	Temp. (°C)	Pressure (psig)	Sweep gas flow rate dry scc/sec	Permeate conc. (ppm)			Permeability (Barrer x 10 <sup>-4</sup> )			Selectivity	
					H <sub>2</sub> S	H <sub>2</sub>	He	H <sub>2</sub> S	H <sub>2</sub>	He	H <sub>2</sub> S/H <sub>2</sub>	H <sub>2</sub> S/He
T-2	11/18/93	560	50	16.7	34	590	210	2.7	2.35	1.67	1.15	1.62
	11/19/93	500	50	16.7	20	400	130	1.62	1.59	1.03	1.02	1.57
	11/21/93	500	50	16.7	12	840	270	0.95	3.34	2.14	0.28	0.44
T-3	11/22/93 <sup>a</sup>	530	50	16.7	20	1,930	620	1.62	7.68	4.92	0.21	0.33
	12/4/93	500	50	16.7	1.8	50	22	0.18	0.24	0.21	0.75	0.86
	12/6/93	516	50	16.7	2.6	85	38	0.25	0.42	0.37	0.6	0.68
T-4	12/16/93	510	50	16.7	0.3	40	15	0.02	0.15	0.11	0.13	0.18
	12/22/93	515	50	16.7	4.4	170	60	0.33	0.64	0.45	0.52	0.73
T-5	12/29/93	515	50	16.7	37	80	22	2.76	0.3	0.16	9.2	17.3
	12/30/93	515	50	16.7	31	85	25	2.31	0.32	0.19	7.22	12.2
	12/30/93 <sup>a</sup>	515	50	16.7	31	112	32	2.31	0.42	0.24	5.5	9.6

<sup>a</sup>At the end of the run.

Coal Gas ~12% H<sub>2</sub>, 6% He, 6% CO<sub>2</sub>, 18% CO, 0.6% H<sub>2</sub>S, and balance N<sub>2</sub>.

night operation, a leak developed in the membrane leading to very high sweep outlet concentrations. The next day the system pressure was reduced to 50 psig returning concentrations to stable levels for the next 20 hours. The H<sub>2</sub>S selectivities with respect to helium and hydrogen were much lower during this period and were about 0.4 and 0.3, respectively. The membrane temperature was then increased from 500 to 530 °C. All the sweep outlet concentrations again began to increase; however, there was not any significant change in the H<sub>2</sub>S selectivities with respect to other gases. The observed H<sub>2</sub>S permeabilities were somewhat lower than those in disc membrane experiments and ranged from 9,500 to 27,000 Barrers.

The concentration and selectivity data collected during this continuous run of over 100 hours are shown in Figures 3-12, 3-13, and 3-14. The continuous rapid increase in the sweep outlet concentrations of both helium and hydrogen at 560 °C as well as 530 °C indicates that above 530 °C molten salt flows downward by gravity within the tube opening up pores in the upper section of the tube. Upon disassembly, salt deposits were observed on both inside and outside of the lower section of the tube, as seen in Figure 3-15(a) and 3-15(b), confirming the salt flow within the tube. The salt is much less mobile at 500 °C, as indicated by relatively stable permeate concentrations of helium and hydrogen. The H<sub>2</sub>S selectivity with respect to helium and hydrogen was low indicating smaller contribution of diffusional H<sub>2</sub>S transport to the overall permeate flow. The potential reasons for the poorer performance of the tubular membranes, as opposed to disc membranes, include (1) downward migration of salt, thereby opening up pores; (2) greater thickness of the tube, thus offering greater liquid phase diffusional resistance; and (3) unimpregnated part of the thickness on the inner side of the tubular membrane which provides additional gas phase mass transfer resistance.

### 3.3.2 Run No. T-3

This run was conducted from 11/30/93 to 12/7/93. During the previous run, rapid increase in helium and hydrogen concentrations was observed indicating downward salt movement within the membrane creating unfilled pores for leakage. Therefore, in this run, the effect of temperature on the molten salt mobility was determined by increasing the temperature gradually in stages starting at 490 °C, just above the salt melting point. A small leak flow through the tube was again observed at 20 psi pressure differential during the cold pressure test. The run began with 30 percent CO<sub>2</sub> on both sides of the membrane at 50 psig pressure. The initial hydrogen leak rate through the tube was determined using a KRW clean coal gas as a feed gas and was found to produce about 45 ppm hydrogen concentration and about 18 ppm helium concentration in the sweep outlet gas. The KRW coal gas with H<sub>2</sub>S was started next. The H<sub>2</sub>S concentration began appearing in the permeate after about 4 hours. Although the operating conditions were stable, frequent surges in all the three concentrations were observed. The temperature was increased to 500 °C over 4 days, with relatively little change in the H<sub>2</sub>S, He, and H<sub>2</sub> concentrations. The H<sub>2</sub>S to helium selectivity reached a maximum of 0.9, eventually leveling off at 0.6. The temperature was then increased to 530 °C in stages to increase the reactivity of H<sub>2</sub>S and salt. The helium and hydrogen concentrations increased steadily with time for temperatures greater than 505 °C. The rate of increase was even greater at temperatures greater than 515 °C indicating downward movement of salt due to gravity. Although the H<sub>2</sub>S concentrations also increased with higher temperatures, the H<sub>2</sub>S to helium selectivity increased very slowly indicating that bulk of H<sub>2</sub>S permeation was associated with the leakage flow.

Although there were frequent surges in the permeate concentrations, because of the lower membrane temperature the baseline permeate concentrations were lower than those observed

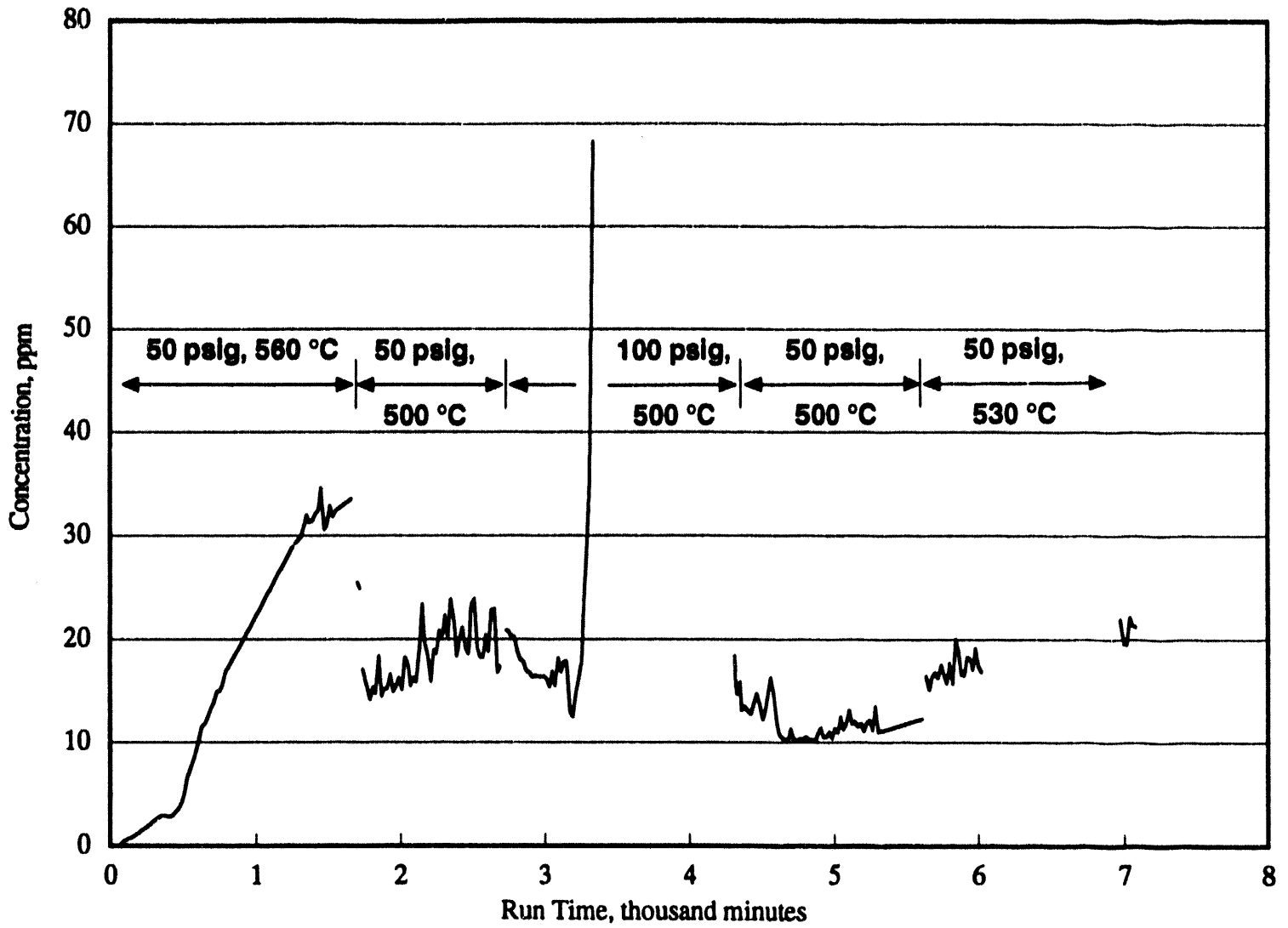


**Figure 3-12. H<sub>2</sub>S concentration with time**  
 (Run T-2, 11/17/93 – 11/22/93, 50, 100 psig, 500 – 560 °C).

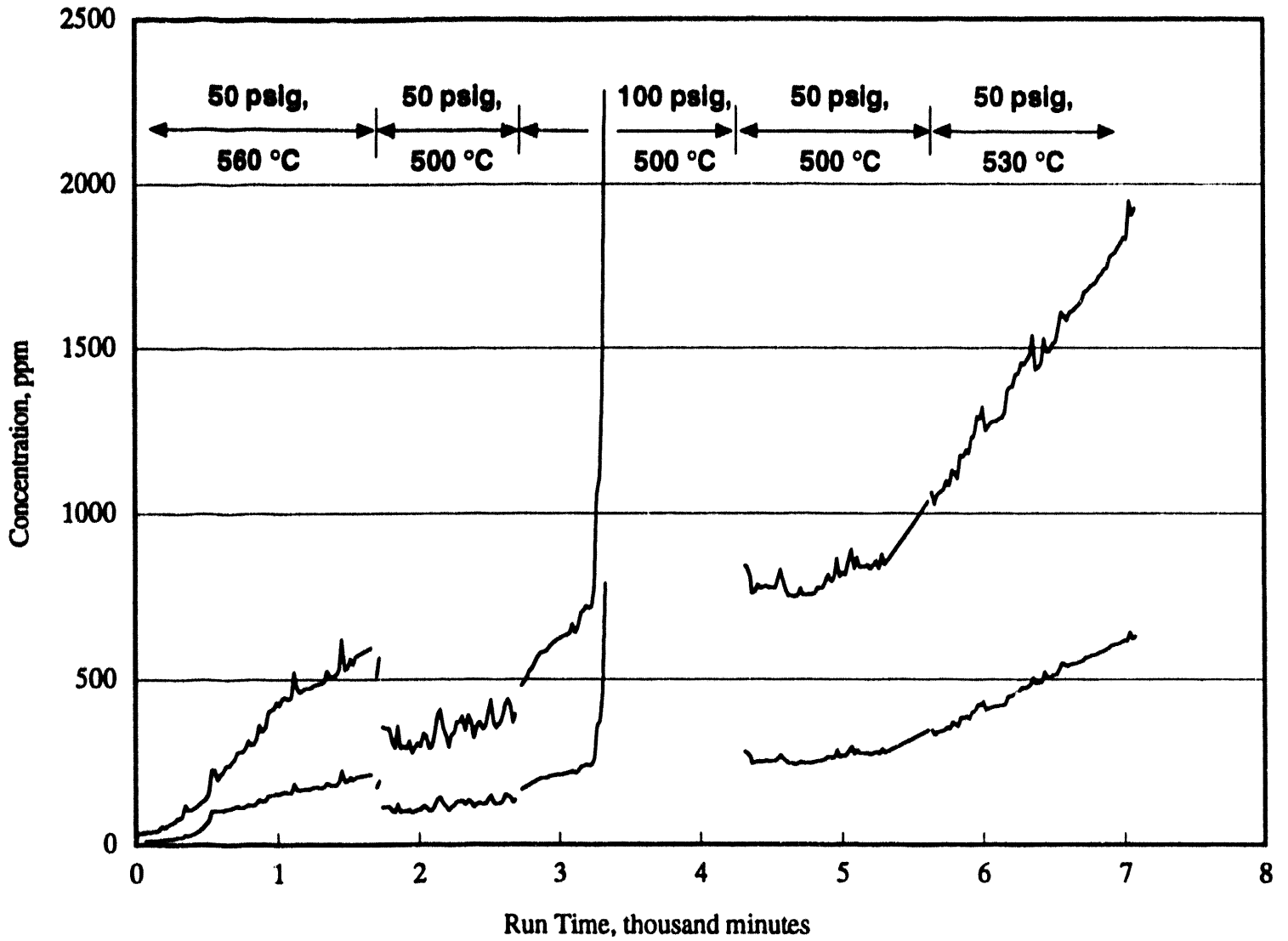


**Figure 3-13. Helium and hydrogen concentration with time (Run T-2, 11/17/93 – 11/22/93, 50, 100 psig, 500 – 560 °C).**



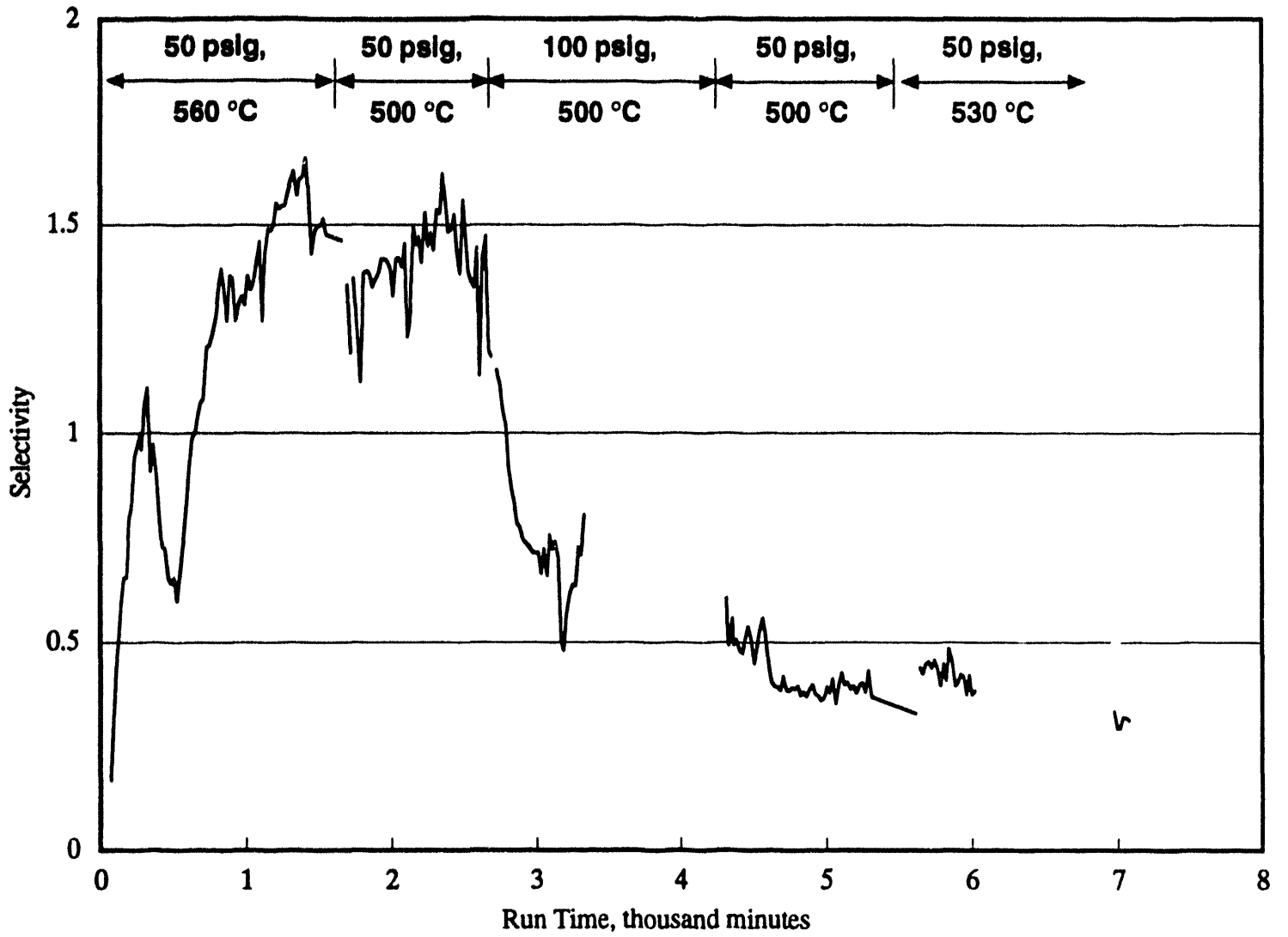


**Figure 3-14. H<sub>2</sub>S/He selectivity with time**  
 (Run T-2, 11/17/93 – 11/22/93, 50, 100 psig, 500 – 560 °C).

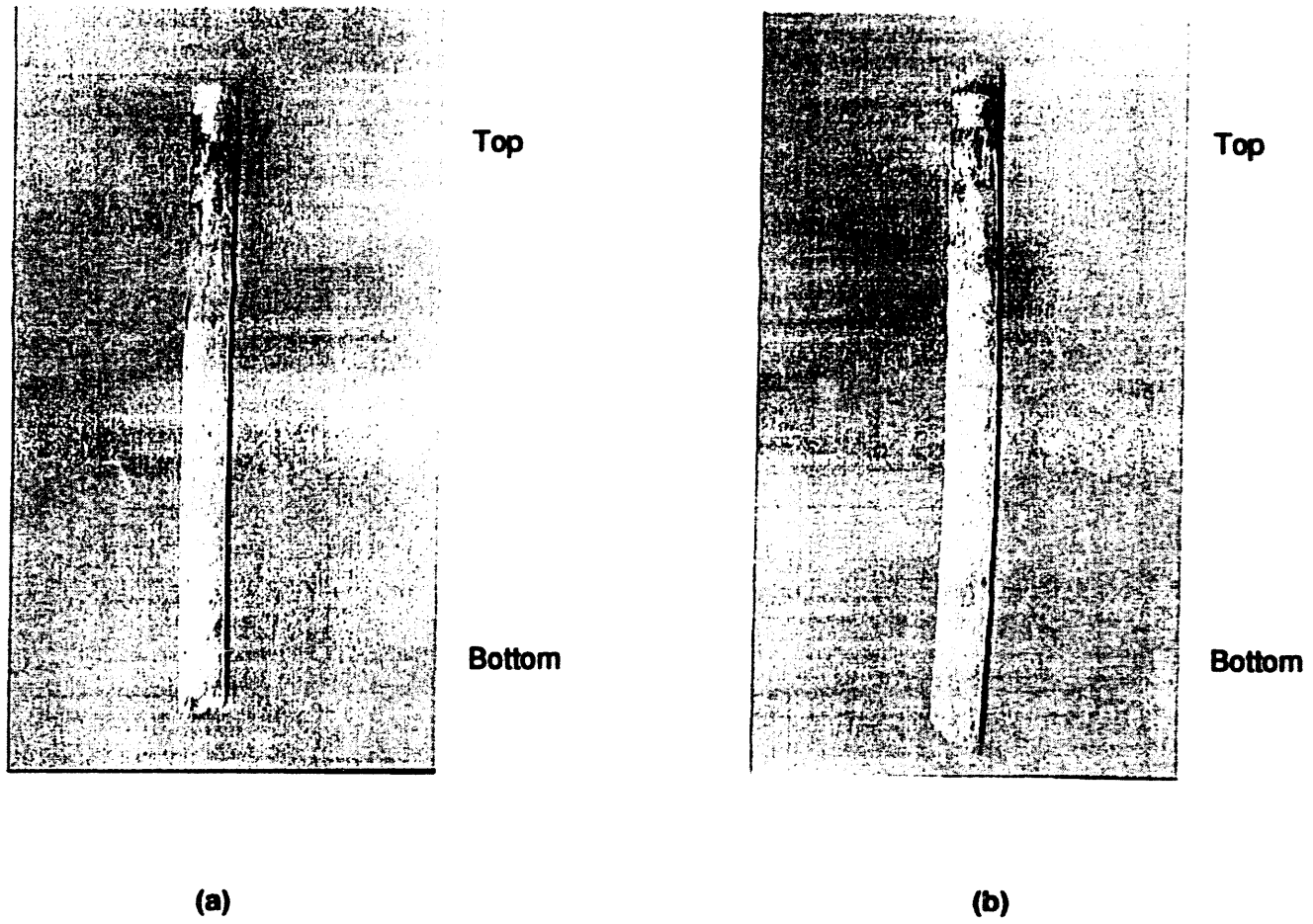


**Figure 3-15. Used tubular membrane showing downward salt movement.**

in Run No. T-2. The H<sub>2</sub>S permeability at the membrane temperatures of 500 to 515 °C ranged only from 1,800 to 2,500 Barrers. The helium and hydrogen permeabilities were also lower than in Run No. T-2.

### 3.3.3 Run No. T-4

This run, with a new membrane, began with 50 psig pressure, 510 °C temperature and KRW clean coal gas on the test side. This run was carried out from 12/15/93 to 12/22/93. The initial porous leak flow produced about 45 ppm hydrogen and 17 ppm helium in the sweep gas. The feed gas was then switched to KRW coal gas with H<sub>2</sub>S. The helium and hydrogen permeate concentrations were very stable initially, while H<sub>2</sub>S concentrations rose very slowly. The selectivity for H<sub>2</sub>S was well below 1, although rising slowly. The temperature was then increased to 520 °C and then decreased to 515 °C to prevent rapid increase in helium and hydrogen permeate concentrations which leveled off at 60 ppm and 170 ppm, respectively. The H<sub>2</sub>S to helium selectivity increased from 0.2 to 0.7 over the 7 days of this run, which indicated substantial leakage flow along with an increasing contribution of the facilitated transport of H<sub>2</sub>S. Similar to Run No. T-3, the H<sub>2</sub>S permeabilities were low because of lower membrane temperatures and ranged from 200 to 3,300 Barrers. The helium and hydrogen permeabilities were also low compared to Run No. T-2, indicating lesser salt movement in the membrane. The continuous increase in the selectivity also indicates that steady state with respect to H<sub>2</sub>S transport had not been reached even after 7 days of this run. The concentrations and selectivities with time during this period are shown in Figures 3-16, 3-17, and 3-18.

At the end of Run No. T-4, the membrane test system was sealed up with 2.9 percent H<sub>2</sub>S in N<sub>2</sub> on the test side and 30 percent CO<sub>2</sub> in N<sub>2</sub> on the sweep side. The steam was turned off on both sides of the membrane. The membrane was then maintained at 510 °C during the 4-day holiday period.

### 3.3.4 Run No. T-5

This run was conducted with the same membrane tube used in Run No. T-4 with coal gas on the test side, 50 psig pressure, and 515 °C temperature; the same conditions at the end of the T-4 run. This run was carried out for 4 days on 12/27-12/31/93. The sealing of the membrane tube at the end of the previous run allowed sulfidation of the salt by the 2.9 percent H<sub>2</sub>S sealed on the test side of the membrane similar to the disc membrane Run No. 6-4. Thus, at the start of this run, H<sub>2</sub>S concentrations in excess of 100 ppm were observed. The H<sub>2</sub>S concentration in the permeate then decreased continuously, eventually leveling off at about 31 ppm. Interestingly H<sub>2</sub> concentration also decreased initially and leveled off before rising again.

This observation indicates some dependence of H<sub>2</sub> transport on H<sub>2</sub>S transport, e.g., decomposition of H<sub>2</sub>S. The helium concentration, on the other hand, first increased slowly, leveled off, and then began rising along with hydrogen concentration. This run was aborted due to a power failure which shut off the furnace. The membrane tube was found to be cracked due to rapid cooling and the membrane run could not be continued. The concentrations and selectivities observed in this run are shown in Figures 3-19, 3-20, and 3-21.

The H<sub>2</sub>S to He selectivity decreased continuously with time from over 100 at the beginning to about 9 at the end of this run. During the same time, the membrane selectivity for H<sub>2</sub>S with respect to hydrogen decreased from about 14 to 6. At the end, although the H<sub>2</sub>S concentration

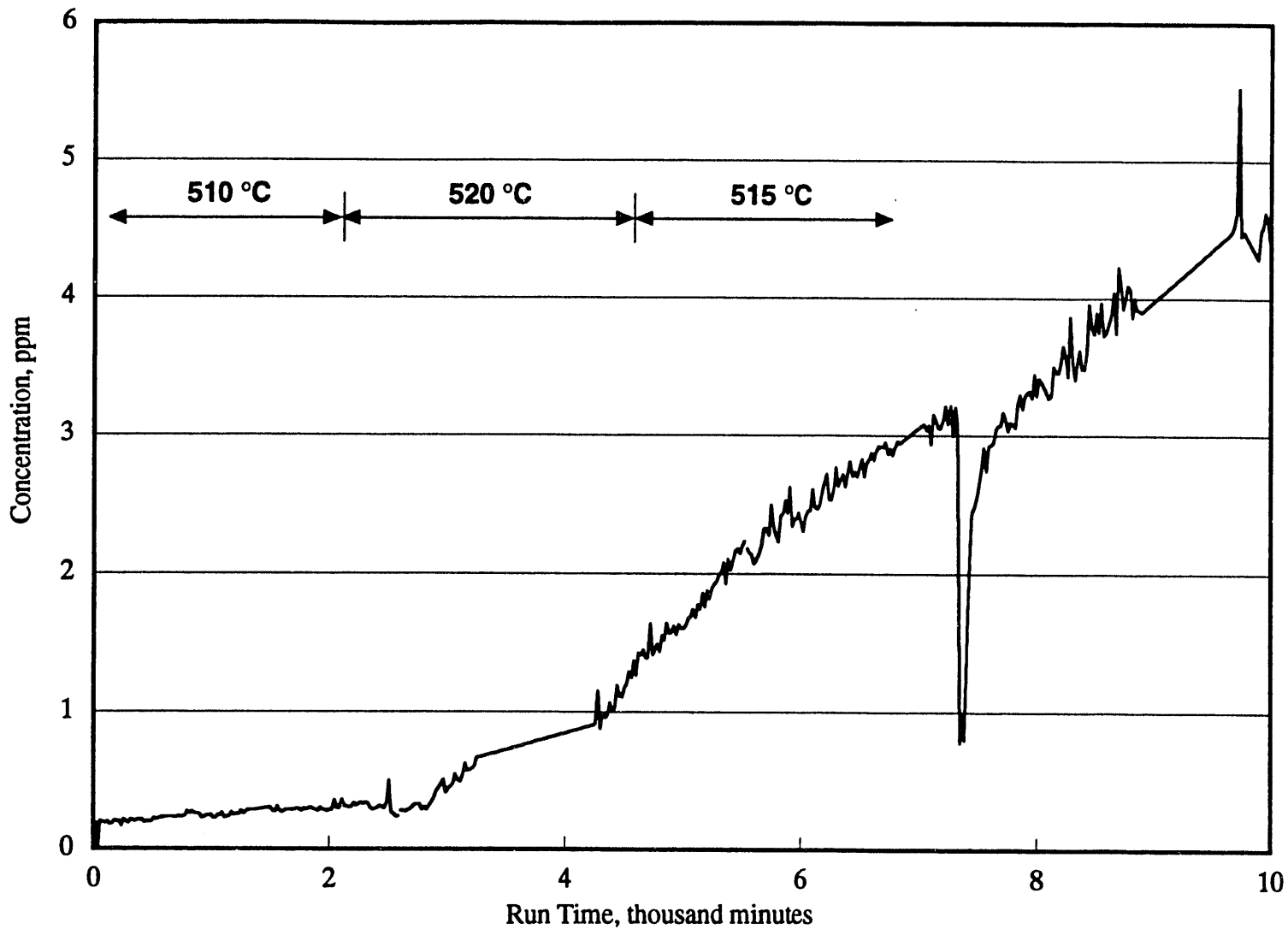


**Figure 3-16. H<sub>2</sub>S concentration with time  
(Run T-4, 12/15/93 – 12/22/93, 50 psig, 510 – 520 °C).**

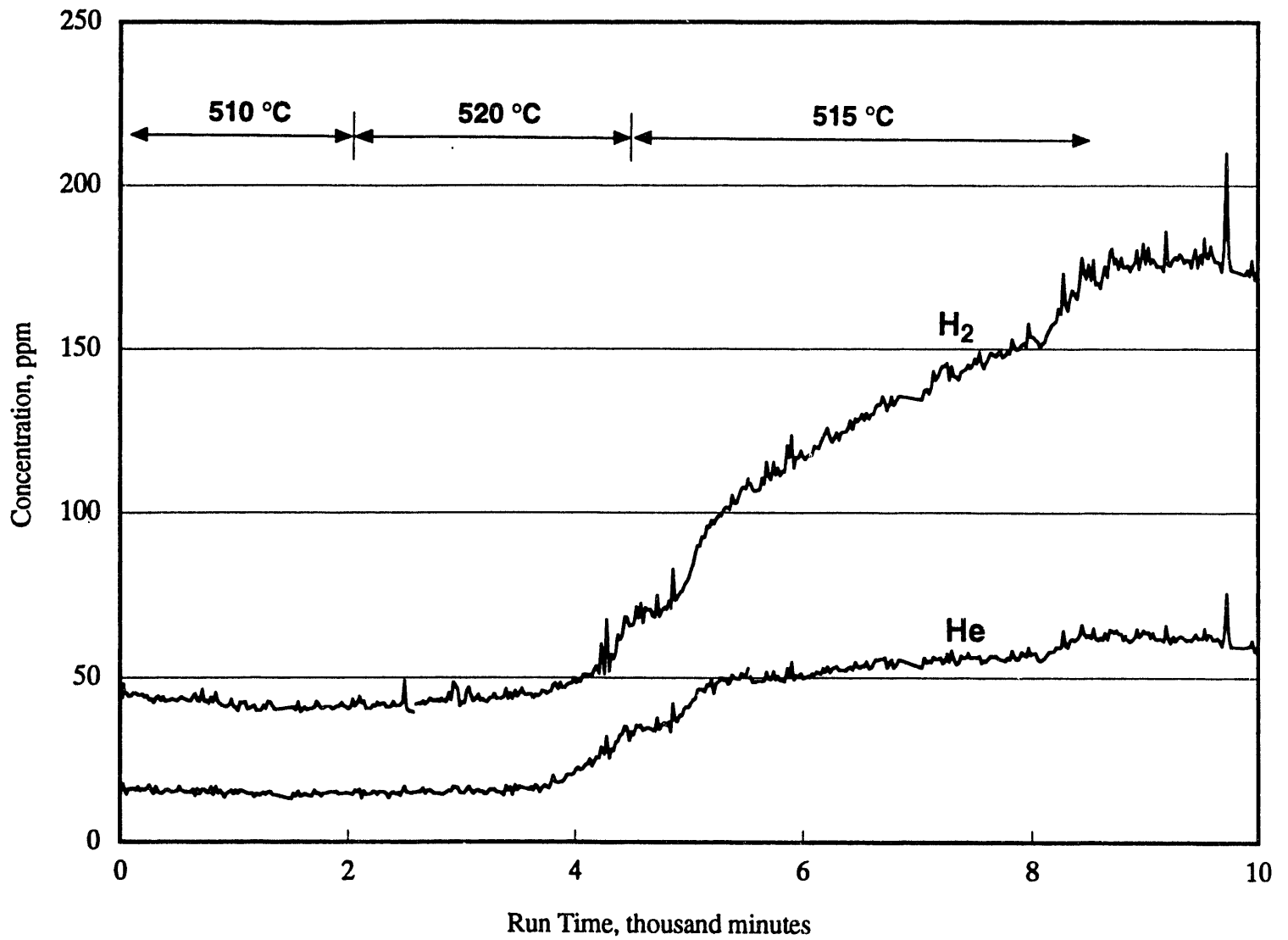


**Figure 3-17. Helium and hydrogen concentration with time  
(Run T-4, 12/15/93 – 12/22/93, 50 psig, 510 – 520 °C).**

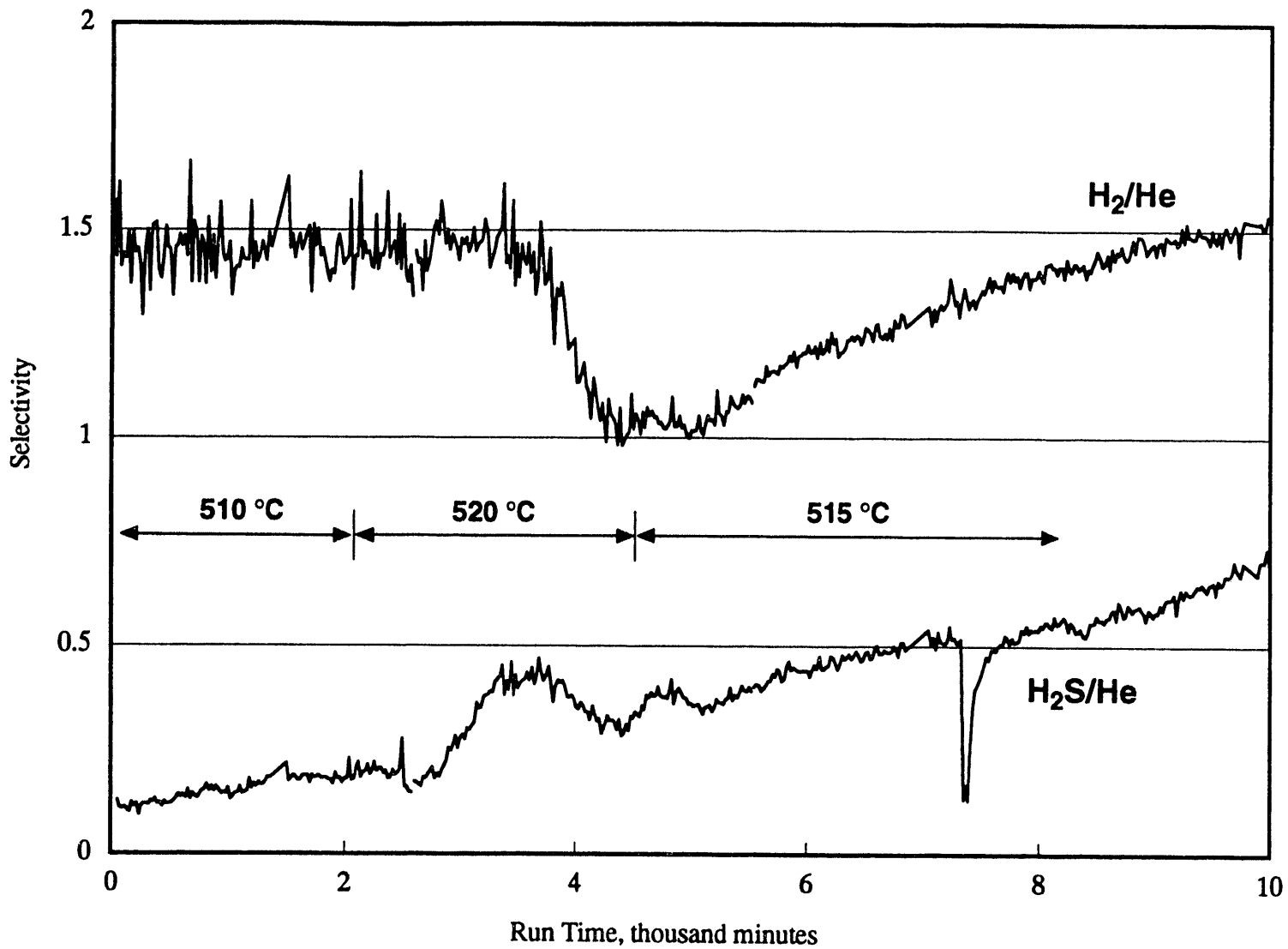
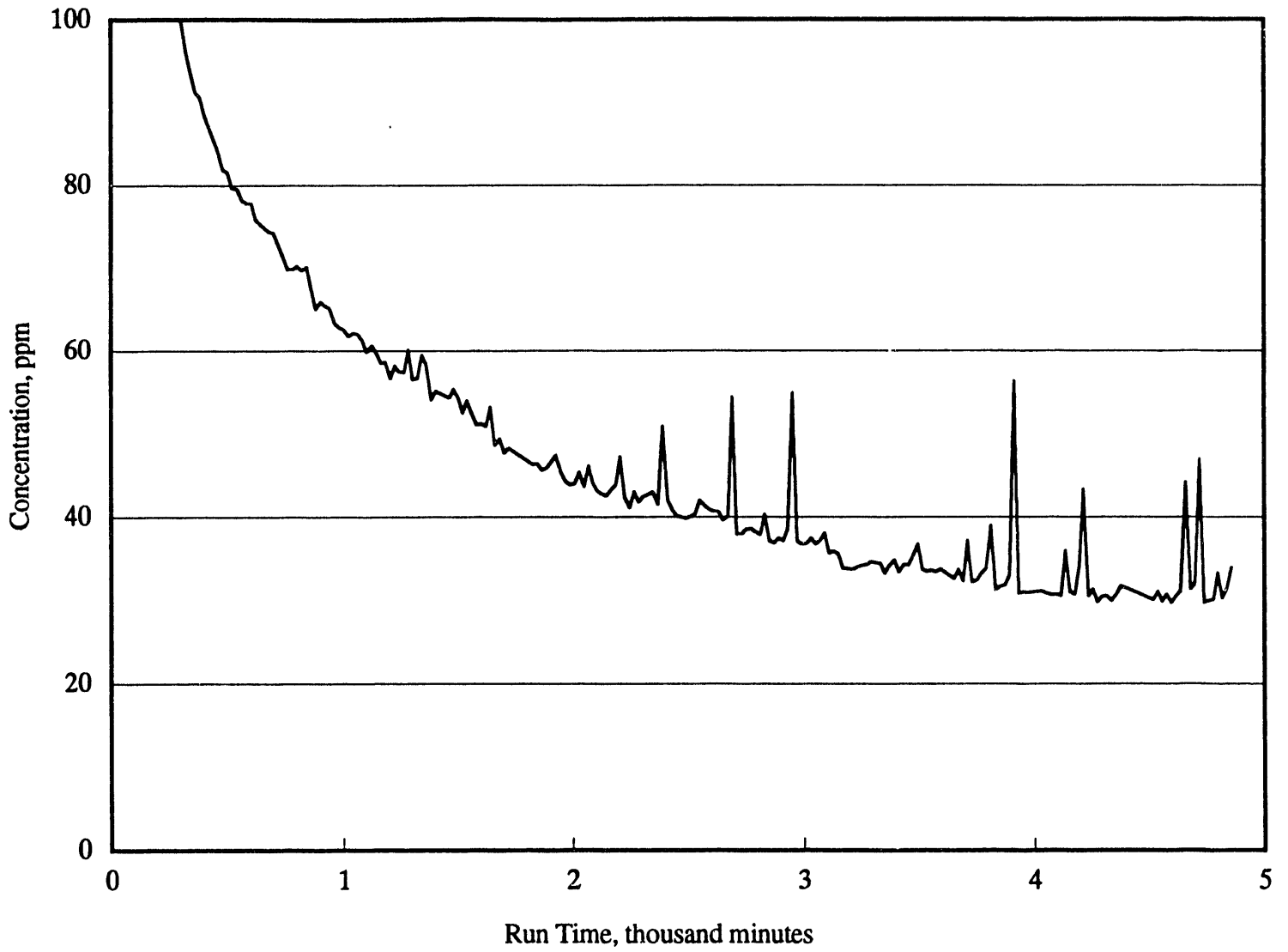
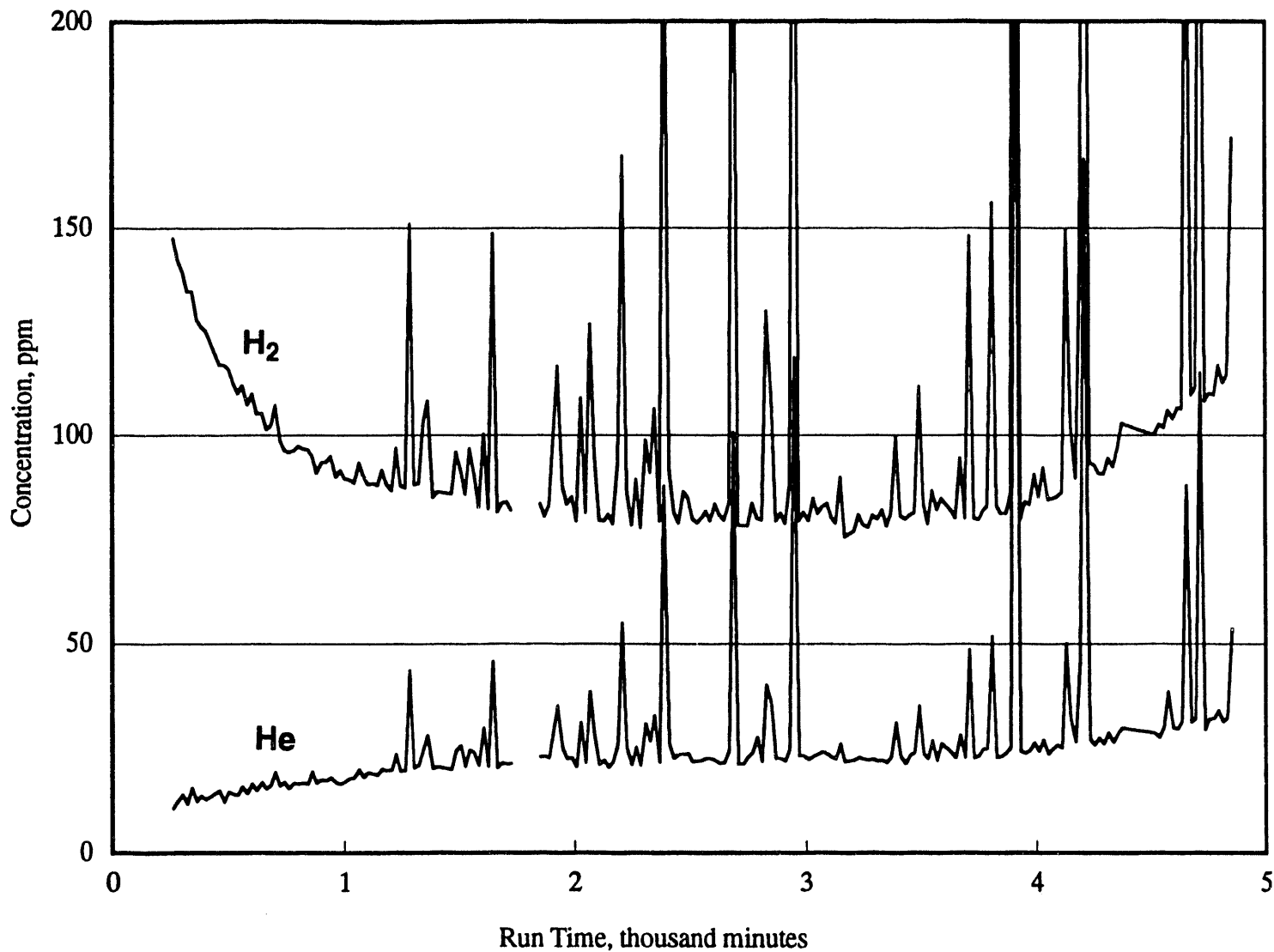


Figure 3-18. H<sub>2</sub>S/He and H<sub>2</sub>/He selectivities with time (Run T-4, 12/15/93 – 12/22/93, 50 psig, 510 – 520 °C).



**Figure 3-19. H<sub>2</sub>S concentration with time  
(Run T-5, 12/27/93 – 12/31/93, 50 psig, 515 °C).**



**Figure 3-20. Helium and hydrogen concentration with time  
(Run T-5, 12/27/93 – 12/31/93, 50 psig, 515 °C).**



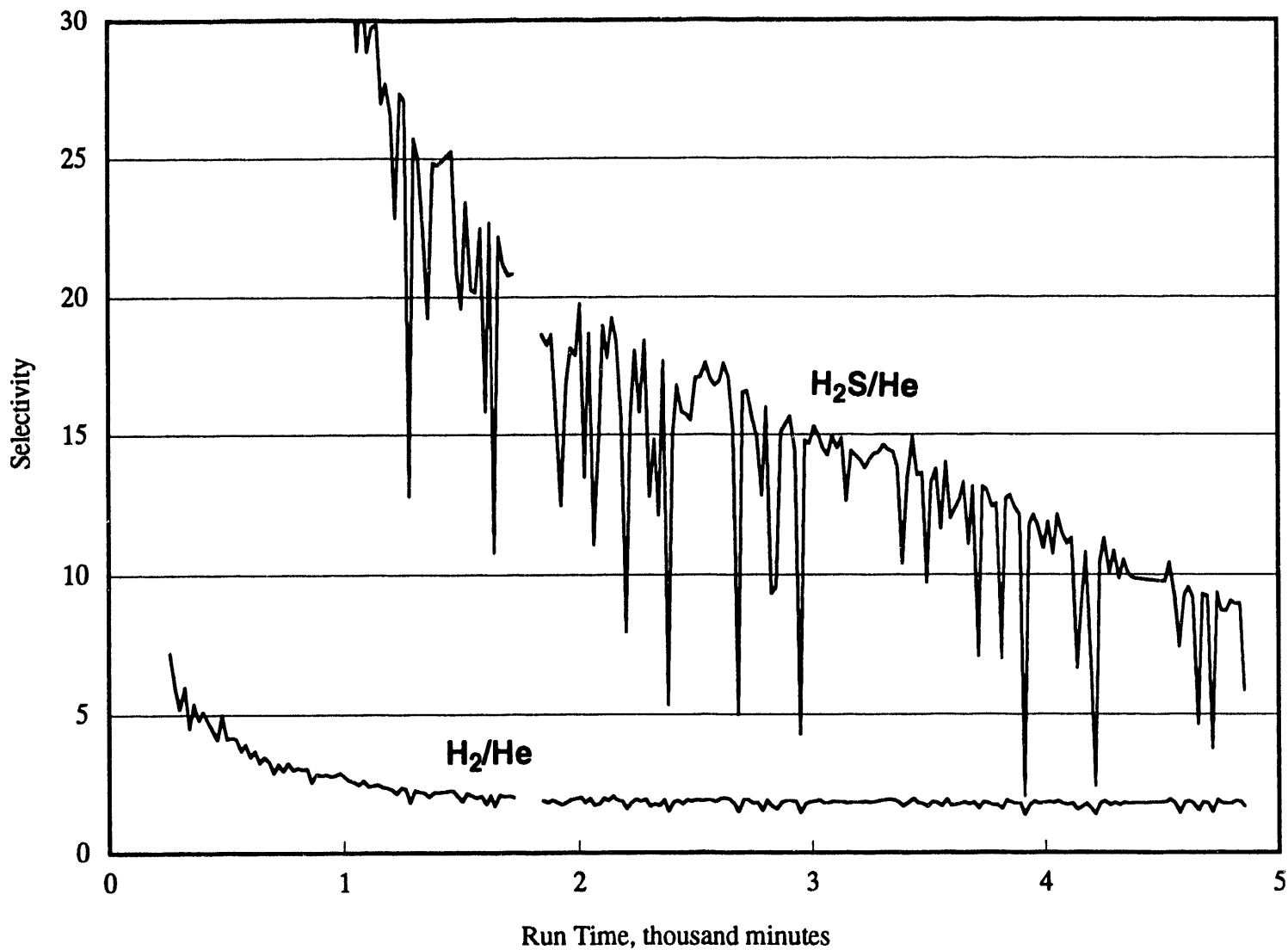


**Figure 3-21.  $H_2S/He$  and  $H_2/He$  selectivities with time (Run T-5, 12/27/93 – 12/31/93, 50 psig, 515 °C).**

had leveled off, the selectivity was still decreasing because of the increasing helium concentration with leakage flow. This run, however, clearly indicated reaction pathway for enhanced H<sub>2</sub>S transport as evidenced by the membrane selectivities for H<sub>2</sub>S, with respect to helium and hydrogen, considerably greater than 1. The H<sub>2</sub>S permeabilities were almost an order of magnitude greater than those observed in Run No. T-4 with the same membrane. At the same time, the helium and hydrogen permeabilities were similar to those in Run No. T-4.

### 3.3.5 Summary and Discussion

Initial experiments (Run No. T-2) with the tubular membranes at a temperature of 560 °C, which was typically used during disc membrane experiments, indicated substantial downward migration of salt by gravity with subsequent opening of pores in the upper section of the tubular membrane. Subsequent testing (Run No. T-3) at lower temperatures indicated that membrane temperature needs to be less than 520 °C to prevent rapid increase in inert gas permeation by leakage. The permeability of the tubular membranes for H<sub>2</sub>S was found to be much lower than those observed in the disc membrane experiments. Possible reasons for the lower H<sub>2</sub>S permeabilities include lower temperatures used in Runs No. T-3 and T-4, larger thickness of the tubular membranes as compared to the disc membranes, and the unimpregnated part of the thickness on the inner side of the tubular membrane which provides additional gas-phase mass transfer resistance.

In Run No. T-4, the membrane selectivity for H<sub>2</sub>S increased continuously over 7 days, which indicated that a steady state had not reached by the end of the 7-day run. Both the membrane permeability and selectivity for H<sub>2</sub>S increased dramatically upon sulfidation of the salt in sealed conditions. Apparently, sulfidation of salt in static conditions helped establish S<sup>2-</sup> concentration gradient within the liquid phase. At the end of Run No. T-5, the concentrations of helium and hydrogen were again on the rise indicative of pore opening with the downward salt movement even at 515 °C membrane temperature. The apparent leveling of H<sub>2</sub>S concentrations resulted from two contrasting factors — increase in H<sub>2</sub>S permeation with porous leakage flow and decrease in permeation due to decreasing S<sup>2-</sup> ion concentrations on the sweep side of the membrane due to continued stripping. Again the relatively long time needed for stripping of the S<sup>2-</sup> from the sweep side of the membrane indicates slow reaction rate and low liquid phase diffusivities at the lower temperatures used in the tubular membrane studies.